THE JOURNAL OF PHYSICAL CHEMISTRY B

Article

pubs.acs.org/JPCB

Self-Aggregation of MEGA-9 (*N*-Nonanoyl-*N*-methyl-D-glucamine) in Aqueous Medium: Physicochemistry of Interfacial and Solution Behaviors with Special Reference to Formation Energetics and Micelle Microenvironment

Animesh Pan, Soumya Sundar Mati, Bappaditya Naskar, Subhash Chandra Bhattacharya, and Satya Priya Moulik*

Centre for Surface Science, Department of Chemistry, Jadavpur University, Kolkata 700032, India

Supporting Information

ABSTRACT: Self-aggregation of MEGA-9 (*N*-nonanoyl-*N*-methyl-D-glucamine), a nonionic sugar-based surfactant, was studied with respect to the effect of salt (NaCl) and ionic liquid (1-butyl-3-methylimidazolium tetrafluoroborate) on its critical micelle concentration (cmc), aggregation number, hydrodynamic dimensions, energetics of micellization, and micellar microenvironment. Fluorimetry (both steady state and time resolved) was used to understand the microenvironments under the influence of additives. NaCl was found to decrease cmc, increase aggregation number (*N*), increase micellar size, and decrease enthalpy of micelle formation; the IL effect on the parameters was mostly opposite. The microscopic properties of micelles were probed using two fluorophores: one nonpolar C-153 (2,3,5,6-1*H*,4*H*-tetrahydro-8-trifluormethylquinolizino-(9,9*a*,1-*gh*)coumarin) and the other fairly polar ANS (8-anilinonaphthalene-1-sulfonate); they delivered information on the palisade layer and the peripheral region of the micelle interface, respectively. Energy of activation and entropy of activation of the dynamics of the probes were evaluated from their decay time, lifetime, and rotational movements in the regions of residency in the micelles. Density functional theory (DFT) calculations showed that the ternary combination MEGA-9/IL/H_2O had the maximum interaction energy compared to any of the binary combinations. Thus, the ionic liquid reduced MEGA-9 self-association to a large extent.

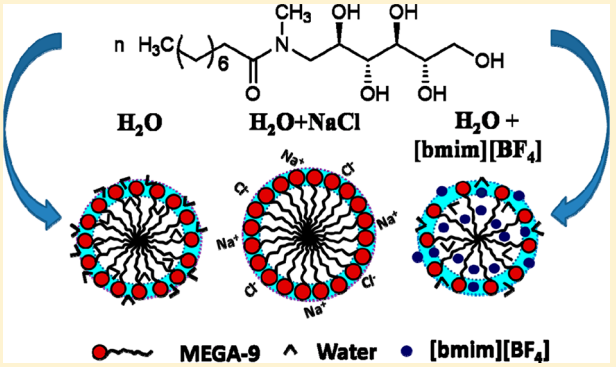

1. INTRODUCTION

Surfactants have attracted attention for their special properties and many fold uses in pharmaceutics, membrane mimetic media, drug delivery, emulsification, nanomaterial synthesis, vesicle formation, oil recovery, etc.[1−9] Controlling environmental conditions, viz., temperature, pressure, and additives (cosolvents, cosurfactants, electrolytes, polar and nonpolar organics, etc.), solution properties of surfactants can be modulated, making them to suit different needs.[10−13] Medium-dependent interfacial and bulk properties of surfactants in relation to thermodynamics and structural properties are also of importance.[11] With the growth of surface chemical research, synthetic surfactants are being extensively used compared to natural occurring amphiphiles. The former class has posed problems being environment unfriendly, making scope for preparation of natural and environment-compatible (biodegradable) amphiphiles.

Sugar-based surfactants have been found to satisfy the aforementioned requirements and are considered to have good potential in colloid and interface science. The nonionic surfactants *n*-octyl-*β*-D-thioglucoside (OTG) and *N*-alkanoyl-*N*-methyl-D-glucamines (MEGA-*n*) are important classes of sugar based surfactants. They are "green" (rapidly disintegrate in environment) and have good dermatological properties.[14] They have relatively higher critical micelle concentration (cmc) than other nonionic surfactants, permitting easier removal (for instance, by dialysis); the small size of their micelles favor their use in gel filtration. They can solubilize proteins without denaturation, have mild temperature-dependent properties, and do not cloud like ethoxylated nonionics.[15−17] Among MEGA-*n*, *N*-decanoyl-*N*-methyl-D-glucamine (MEGA-10) is conventionally used in solubilizing membrane proteins. Its physicochemistry has been fairly studied.[18−27] Compared to MEGA-10, the next lower homologue, *N*-nonanoyl-*N*-methyl-D-glucamine (MEGA-9), is much less studied, although it is also a good membrane solubilizer and forms vesicles.[28−30] A detailed physicochemical study of MEGA-9 is thus considered worthy.

The alkyl glucosides and glucamines show differences in their solution properties because of the rigidity differences between their head groups. The former has more rigid heads than the

Received: January 5, 2013
Revised: May 7, 2013

dx.doi.org/10.1021/jp400139d | *J. Phys. Chem. B* XXXX, XXX, XXX−XXX

latter, hence salt- and temperature-induced dehydration of the latter class is less probable than the former. Therefore, variants like salt (both concentration and type), temperature, added solvents, and other additives (urea, polyols, carbohydrates, etc.) make distinct differences in their solution properties. Hierrezuelo et al.[19] and Molina-Bolivar et al.[20] have made detailed studies on OTG and MEGA-10 by way of salt and temperature effect on their assembly formation exploring micellar size, shape, aggregation number, viscosity, micelle local properties (polarity, viscosity, etc.): these are useful and important contributions in the field of colloid and surface chemistry. Okuwauchi et al.[22] made a physicochemical study on MEGA-8, MEGA-9, and MEGA-10. Their self-assembly, temperature effect on cmc, and effect of chain length and different groups of the molecules on the thermodynamic parameters were evaluated. Nature of their assemblies was also attempted to understand by static light scattering method. But investigations on their macroscopic and microscopic properties in detail remained unexplored.

Since MEGA-*n* classes of sugar-based surfactants have not been adequately studied, we have herein investigated detailed solution properties of one of its poorly studied representative, MEGA-9. The following aspects with reference to its self-association in solution have been examined: (1) micelle formation in the presence of varied concentrations of the salt NaCl and room temperature ionic liquid, IL (1-butyl-3-methylimidazolium tetrafluoroborate, [bmim][BF_4]); (2) effect of temperature on micelle formation and analysis of data based on enthalpy of micellization by van't Hoff method and that by calorimetry; (3) DLS and viscosity measurements to determine the shape and size of the micelle formed in the presence of salt and IL as well as at varied temperatures; (4) micelle aggregation number and its microproperties like polarity, viscosity, and quencher−probe complexation and their distribution and rotational dynamics by static and time-resolved fluorescence measurements; and (5) understanding of physical-chemical affinity of MEGA-9 with IL and water by density functional theory (DFT) calculations.

2. EXPERIMENTAL SECTION

2.1. Materials and Methods. The MEGA-9 (*N*-nonanoyl-*N*-methyl-D-glucamine) used was a product of Dojindo Laboratories, Kumamoto, Japan. Pyrene and CPC (cetylpyridinium chloride) were purchased from Sigma-Aldrich. C-153 (2,3,5,6-1*H*,4*H*-tetrahydro-8-trifluormethylquinolizino-(9,9*a*,1-*gh*)coumarin) and ANS (8-anilionaphthalene-1-sulfonate) (laser grade, Exciton) were used as received. NaCl (AR grade) was of Merck (India); GH (guanidine hydrochloride) and 1,4-dioxane were AR grade of Spectrochem (India), and the room temperature ionic liquid, IL (1-butyl-3-methylimidazolium tetrafluoroborate, [bmim][BF_4]) with stated purity of higher than 98.5% mass fraction, was obtained from Sigma-Aldrich and was dried under vacuum at 30 °C for 12 h to remove moisture before use. Doubly distilled conductivity water (specific conductance, κ = 2−3 μS cm^{-1} at 303 K) was used in the experiments.

2.1.1. Spectral Measurements. Absorption spectra were taken using a Shimadzu UV-1601 (Japan) spectrophotometer at the desired temperature using quartz cuvettes of 1 cm path length.

Steady-state fluorescence measurements were performed using a Perkin-Elmer LS 55 (USA) fluorescence spectrophotometer with an attachment of Fluorescence Peltier System PTP-1 using a glass cell of 1 cm path length.

Steady-state fluorescence anisotropy (r_{ss}) measurements were taken with a polarization filter having the "L-format" configuration to measure the r_{ss} (fluorescence anisotropy) of the probes C-153 and ANS. The anisotropy relation is expressed as[31]

$$r_{ss} = \frac{I_{VV} - GI_{VH}}{I_{VV} - 2GI_{VH}} \quad (1)$$

and

$$G = \frac{I_{HV}}{I_{HH}} \quad (2)$$

where I_{VV} and I_{VH} are the vertically and horizontally polarized emission intensities, respectively, resulting from vertically polarized excitation of the probe. In the expression for the *G* factor, I_{HV} and I_{HH} are similarly the vertically and horizontally polarized emissions resulting from horizontally polarized excitation, respectively. The anisotropy values were averaged over an integration time of 20 s, and a maximum of three measurements were taken for each sample. The anisotropy values of the probe in micellar media as presented in this work are the mean value of three individual determinations.

The steady-state fluorescence quenching method was used for the determination of mean micelle aggregation number (*N*). In all experiments, CPC was used as the quencher. Working solutions containing ∼1.2 μM pyrene and 200 mM of surfactant were prepared in pure water, and in NaCl and IL solutions of different concentrations. [Quencher] in solution was maintained low enough (1 μM) to not perturb the micelle assembly. The slit widths of excitation and emission were 9.0 and 4.0 nm, respectively; the scan speed was 250 nm/min. Emission spectra were recorded between 350 and 500 nm using excitation at λ = 333 nm.

Cmc values were obtained through sigmoidal[32] fitting and the micelle aggregation number (*N*) was obtained from the following relation:[33,34]

$$\ln\left(\frac{I_0}{I_Q}\right) = \frac{N[\mathrm{CPC}]}{[\text{MEGA-9}] - \mathrm{cmc}} \quad (3)$$

where I_0 and I_Q are the fluorescence intensities of pyrene in the absence and presence of quencher CPC, respectively; [MEGA-9] is the total concentration of the surfactant in solution which was kept constant, and [CPC] is the concentration of quencher in the system which was varied. The slope of the linear plots between $\ln(I_0/I_Q)$ versus [CPC] yielded the mean aggregation number (*N*) of the micelles.

2.1.2. Time-Resolved Fluorescence Measurements. Fluorescence lifetimes of ANS and C-153 in different mediums were determined from time-resolved intensity decays by the method of time-correlated single-photon counting (TCSPC) using nanosecond diode excitation sources at 431 nm (IBH, UK, nanolLED-17, nanoLED-07) and TBX-04 as the detector. The instrument response time was ∼1 ns. The decays are deconvoluted using IBH DAS-6 decay analysis software. The quality of the fits was judged by the reduced χ^2 criterion and the randomness of the fitted function to the raw data. Intensity decay curves were fitted as a sum of the exponential terms

dx.doi.org/10.1021/jp400139d | J. Phys. Chem. B XXXX, XXX, XXX−XXX

$$I(t) = \sum_i A_i \exp\left(\frac{t}{\tau_i}\right) \quad (4)$$

where A_i is a pre-exponential factor of the component i with a lifetime τ_i. From these two component contributions, average lifetimes $\langle\tau\rangle$ were calculated using the following equation:[31]

$$\langle\tau\rangle = \frac{\sum_i A_i\tau_i^2}{\sum_i A_i\tau_i} \quad (5)$$

The relative concentration or fractional amount of each component, α_i, was determined from the relation

$$\alpha_i = \frac{A_i}{\sum_i A_i} \quad (6)$$

2.1.3. Isothermal Titration Calorimetry (ITC). An OMEGA ITC microcalorimeter (Microcal, USA) was used for thermometric measurements. A desired concentrated solution of MEGA-9 taken in a 325 μL microsyringe was injected for a duration of 30s into 1.325 mL of solvent (pure water, NaCl, and IL solution) in the calorimetric cell at equal time intervals (210 s) in multiple steps (32−50 additions) under constant stirring (350 rpm) condition. All measurements were taken under thermostated conditions maintained by a Nesleb RTE 100 circulating water bath. The ITC experiments were done in the temperature range of 293−323 K with a precision of ±0.1 K. The heat released or absorbed at each step of dilution of surfactant solution in either water or NaCl and IL solution with different concentrations was recorded, and the enthalpy change per mole of injectant was calculated with the ITC Microcal Origin 2.9 software. The reproducibility was checked from repeat experiments. The enthalpy−concentration profile produced first-order transition in the pattern.

Cmc and enthalpy of micellization (ΔH°_m) were determined from the ITC thermograms. The rationale for getting the cmc and ΔH°_m are found in the literature[35] which is shown in the thermogram in the Supporting Information, Figure SM1. The cmc was the inflection point in the thermogram or the maximum/minimum of its first derivative, and ΔH°_m was the difference between the upper and lower inflection points A and B.

2.1.4. Dynamic Light Scattering Experiment (DLS). The hydrodynamic radius of micelles, R_h, was obtained from light scattering measurements at $\theta = 90°$, which were taken using a Zeta Sizer Nano-S (Malvern, UK) instrument. The instrument has a back-scattering detection device and equipped with a He−Ne laser source (wavelength 632.8 nm) and a Peltier thermoelectric detection system. All the experimental solutions were filtered 2−3 times through membrane filters (pore size 0.25 μm) to remove extraneous matter. The mean values of reproducible experimental results were considered. Errors in the measured hydrodynamic radius were within ±3%.

2.1.5. Viscometry. An Ubbelohde viscometer of 103.6 s average flow time for 10 mL of water at 303 K was used in the study. It was placed in a thermostated water bath with temperature accuracy of ±0.1 K. The MEGA-9 solutions (10 mL) without and with additives were taken in the viscometer and the flow times were measured after thermal equilibration.[36] Each set of measurements was duplicated and their flow times were found to be close. The mean values were recorded and used. The densities of solutions with and without MEGA-9 were also determined to get the relative viscosities of the MEGA-9 solutions at 303 K. Errors in measurements were within ±0.5%.

2.1.6. Tensiometry. A Krüss (Germany) tensiometer was used for surface tension measurements by the ring detachment method. A concentrated solution of MEGA-9 (20 times cmc) was used in thermostated water, salt, and IL solution with a Hamilton microsyringe taking measurements 5 min after addition and thorough mixing and temperature equilibration. Duplicate measurements were used to check reproducibility. The accuracy of measurements was 0.1 mN m^{-1}. Surface tension (γ) vs log[surfactant] was used to get cmc from the breaks in the plot. The γ values were used in Gibbs adsorption equation to evaluate the surface excess at cmc (Γ_{max}).

3. RESULTS AND DISCUSSION

3.1. Micelle Formation of MEGA-9 in NaCl and IL. Two methods fluorimetry (Fl) and calorimetry (ITC) were used to determine the critical micelle concentration (cmc) and other micelle characteristics (polarity index and enthalpy of micelle formation (ΔH°_m)). From the dependence of the fluorescence emission ratio of peak 1 and 3 (F(1:3)), and the enthalpy of dilution in an isothermal titration calorimeter, the cmc of MEGA-9 in aqueous medium in the presence of varied concentrations of NaCl and the IL([bmim][BF_4]) were determined. The results are presented in Tables 1 and 2. The cmc by fluorimetry was found to be lower than that by calorimetry; on the average a difference of 5.4 mM (or 25%) was observed. Higher values of cmc by ITC are often reported in the literature.[23] Using static light scattering, tensiometry and fluorimetry measurements, the cmc of MEGA-9 in the range of

Table 1. Different Physicochemical Parameters for MEGA-9 Micelles As a Function of NaCl and IL [bmim][BF_4] Concentration at 303 K[a]

Section A						
		cmc/mM				
additives	concn (M)	(1:3) ratio	calorim	R_h (nm)	N ($K_{SV} \times 10^{-5}$)	ΔH°_m[b]
NaCl	0	19.8	25.1	2.42	87 (6.02)	5.82
	0.1	19.0	24.6	2.49	83 (5.71)	5.06
	0.5	15.4	20.8	2.58	94 (6.78)	4.60
	0.8	12.8	18.2	2.73	107 (7.73)	4.39
	1.0	11.2	16.4	2.94	128 (9.09)	3.96
[bmim][BF_4]	0.1	23.9	30.3	2.52	73 (5.12)	3.08
	0.5	28.3	38.8	2.65	65 (4.29)	−0.79
	0.8	51.9	56.4	2.49	48 (3.25)	−2.20
1,4-dioxane[c]	2	–	30.2	–	–	4.01
	5	–	38.4	–	–	0.79
	8	–	50.1	–	–	−0.28

Section B[d]			
medium	cmc/mM	A_{min}/nm^2 molecule^{-1}	$\Gamma_{max} \times 10^6$/mol m^{-2}
water	20.5	0.61	2.73
0.5 M NaCl	13.1	0.79	2.01
0.5 M GH	20.7	0.78	2.10

[a]From tensiometry the cmc of MEGA-9 was found to be 20.5 mM at 303 K. [b]Enthalpy changes in micellization (ΔH°_m) are expressed in kJ mol^{-1}. [c]Concentration of dioxane in vol %. [d]The relations used for calculation of different parameters are $\Gamma_{max} = -(1/(2.303iRT))\text{-}\lim_{C\to cmc}[(d\gamma)/(d\ \log C)]$ and $A_{min} = 10^{18}/(N_A\Gamma_{max})$.

dx.doi.org/10.1021/jp400139d | J. Phys. Chem. B XXXX, XXX, XXX−XXX

Table 2. Different Physicochemical Parameters for MEGA-9 Micelles As a Function of Different Temperatures

	cmc/mM			
T/K	(1:3) ratio	calorim	R_h (nm)	N ($K_{SV} \times 10^{-5}$)
293	20.8	26.7	2.46	83 (5.70)
298	–	25.6	–	–
303	19.8	25.1	2.42	87 (6.02)
308	–	24.6	–	–
313	19.5	24.0	2.31	80 (5.49)
318	–	24.0	–	–
323	20.6	24.3	2.19	84 (5.78)

13–25 mM were reported in the past.[28] By tensiometric measurements in aqueous medium, we have found a cmc of 20.5 mM at 303 K. The herein reported cmc values were reproducible and satisfied the range documented in the literature.

Salt effect on MEGA-*n* was hardly studied earlier. The results with NaCl and IL are herein presented, which in our consideration, are the first of their kind. NaCl showed a "salting out" type effect and decreased the cmc of MEGA-9. A decrease in cmc by 42.4% was caused by 1.0 M NaCl. The salt disrupted the hydrophilic hydration of the nonpolar tail and the solvation of the −OH-containing head groups of MEGA-9, causing easier self-organization of the amphiphile. The amphiphile activity declined in salt medium and it was salted out to form assemblies at lower concentration. On the other hand, IL significantly increased cmc. Addition of 0.8 M IL increased cmc 2.6-fold. Behera et al.[37] and Rao et al.[38a] have reported effect of ILs on aggregation of conventional ionic and zwitterionic surfactants; their effects on the behavior of nonionic surfactants are not much studied.[38b,39] However, there was report of decrease of cmc of sodium dodecyl sulfate (SDS) at low concentration and increase at high concentration of IL.[38e] ILs were also found to mildly affect the cmc but make appreciable structure modification of the micelle.[38] So, the effect of ILs on cmc is not unidirectional. The methyl and butyl moieties in the cationic part of the IL ([bmim][BF_4]) acted as cosolvent for MEGA-9, making it compatible with the mixed solvent medium restricting self-aggregation with increased cmc.

In the literature, additive effect on cmc has been often found to correlate in terms of a simple linear relation[11] like

$$\log \text{cmc} = \log \text{cmc}_0 + k \log[\text{A}] \quad (7)$$

where A represents the additive, k is a constant (the slope of the linear relation), and cmc_0 is the cmc without additive. Normally, cmc_0 decreases by the addition of both electrolytes and nonelectrolytes hence a negative slope results.

For ionic surfactants, counterion binding extent of micelles (β) can be found from a similar relation

$$\log \text{cmc} = \log \text{cmc}_0 - \beta \log(\text{cmc} + C_S) \quad (8)$$

where C_S is the concentration of the added counterion (for 1:1 electrolyte C_S = [salt]). This is well-known Corrin–Harkins relation[40] used to determine β, an important physicochemical parameter of ionic micelles. It is known that cmc always decreases with increased [counterion] and hence the slope is negative (as mentioned above). On this physical-chemical basis the above eqs 7 and 8 are complementary. We have plotted log cmc of MEGA-9 against log [NaCl] (Figure 2A) and found a straight line (with good correlation) having an intercept ≡ log cmc_0 and the slope k = −0.254 with fluorimetry cmc data, and k = −0.194 with microcalorimetric cmc data. For the IL (Figure 2B), the courses were nonlinear and in the positive direction; they fitted well to two-degree polynomial relations given in the legend. The property difference of IL from the normal strong electrolyte NaCl was evident. The nonlinear courses meant changed (increased) k by changing [IL] which was a single value both in water and NaCl solution. Addition of IL had a continued hindrance to MEGA-9 aggregation.

The γ–log[MEGA-9/mM] isotherms are presented in the Supporting Information (Figure SM2); the adsorption parameters in water and in 0.5 M NaCl and 0.5 M GH at 303 K are presented in Table 1, section B. The low value of A_{min} = 0.61 nm^2/molecule suggested that the headgroup of MEGA-9, $-CH_2CONCH_3CH_2(CHOH)_4CH_2OH$, assumed a perpendicular configuration at the interface (the value for Triton X-100 with 9.5 POE headgroup produced an A_{min} value of 0.91;[41] *n*-octyl-β-D-thioglucopyranoside produced a value of 0.53;[42] for Tween-20[43] and *n*-nonanoyl-β-D-thiomaltoside,[44] the reported values were 1.41 and 0.43 nm^2/molecule, respectively). The A_{min} values of MEGA-10 in aqueous and 1 M NaCl solution were found to be 0.53 and 0.59 nm^2/molecule, respectively, at 303 K.[20] They were fairly comparable. Molina-Bolívar et al.[20] did not mention the way the slope at cmc was estimated to get Γ_{max} from Gibbs equation. In their report, plots of γ versus log[MEGA-10] were nearly linear but which in our case of MEGA-9 were distinctly sigmoidal. We used a two-degree polynomial fitting[45] to get the required slope $d\gamma/d \log C$ at cmc from the first differential of the polynomial. The procedure for getting the slope at cmc of the γ versus log C plot has a say on the evaluation of Γ_{max} and hence the A_{min} from the Gibbs adsorption equation. The method herein used was considered more appropriate[45,46] for the evaluation of Γ_{max} and A_{min}.

3.2. DLS, Viscosity, and Aggregation Number of Micelles. The shape, size, and aggregation number are important structural parameters of micelles like other disperse species. We have attempted to characterize MEGA-9 micelles by three different methods which are discussed in what follows.

Viscosity is a potential method for understanding the configuration of a disperse species in solution. Spherical bodies have low viscosity; ellipsoids have moderately high viscosity; rod, helical, and elongated configurations produce high viscosity and they can even form gels. η_r (relative viscosity) of MEGA-9 versus total concentration (C) minus cmc or C–cmc plots yielded nice linear courses in water, 0.8 M IL, and 1.0 M NaCl, suggesting unchanged geometry of the micellar dispersion. The relative viscosity at the maximum studied concentration of MEGA-9 (0.15 M or 8cmc) was on the average low (1.33), and the micelles were of globular type. The plots are presented in Figure SM3 in the Supporting Information.

DLS measurements at 2cmc of MEGA-9 yielded hydrodynamic radius (R_h) of the micelles which are presented in Table 1 and the representative plots in Figure SM4 in the Supporting Information. In the presence of NaCl, R_h increased since salt is known to decrease cmc and increase the micelle size. In the case of IL, R_h remained practically unaltered. In the IL medium, cmc of MEGA-9 increased, consequently a decline in micelle size was anticipated which was not reflected on the R_h values; it only modestly increased instead of a decrease. This suggested penetration of nonpolar IL cation and water into the palisade layer of the micelle, causing only a minor size increase.

dx.doi.org/10.1021/jp400139d | J. Phys. Chem. B XXXX, XXX, XXX–XXX

Micelle aggregation number (N) was determined by static fluorescence quenching method along with the determination of Stern–Volmer constant (quencher-probe binding constant, K_{SV}). Representative plots are shown in Figure SM5 in the Supporting Information, and the results are presented in Table 1. The N values were found to increase with NaCl addition; a 1.5-fold increase was observed at 1 M NaCl. The increase in N was in line with the salting out effect as mentioned in relation to the discussion on NaCl effect on cmc. On the other hand, IL decreased N; 0.8 M IL caused a 1.9-fold decrease in N, although R_h had a modest increase. Penetration of IL into the peripheral region of MEGA-9 micelle was further supported. Solvent effect is known to decrease the N of micelle.[13b]

Both cmc and R_h of MEGA-9 micelles decreased with temperature (Table 2). The breakdown of water structure by temperature increment assisted micelle formation (by desolvation and salting out effect) with mild decrease of both cmc and R_h. On the other hand, N remained on the average constant. Constant N with decreasing R_h with elevation of temperature resulted from folding of the desolvated head groups of monomers in the micelle. Above 318 K a tendency of cmc increase was observed by both fluorimetry and calorimetry. At higher temperature, thermal energy opposed monomer aggregation and increased cmc. The cmc–temperature profile very often produces a minimum. The results in Table 2 suggested a minimum around 318 K in aqueous medium. In comparison, MEGA-10 produced a distinct minimum (at 313 K) in its cmc–temperature profile.[23] Its N and R_h were reported[20] to be 76 in water (111 in 1 M NaCl) and 2.6 nm in water (3.2 nm in 1 M NaCl), respectively.

3.3. Energetics of Micellization (ΔH°_m) Based on Indirect Method of van't Hoff and Direct Method of Calorimetry. The cmc data of the nonionic amphiphile MEGA-9 can be used to find out the standard Gibbs free energy change of micellization by the relation

$$\Delta G^\circ_m = RT \ln X_{cmc} \quad (9)$$

where X_{cmc} is the cmc expressed in the mole fraction scale. The cmc results at different temperatures (293–323 K) are presented in Table 3. Column 5 in Table 3 shows ITC determined enthalpy (Figure 1F) values; the endothermic enthalpies declined with temperature and became exothermic. Using the ΔG°_m and ΔH°_m values, the standard entropy of micellization ΔS°_m values of MEGA-9 (calculated from the Gibbs–Helmholtz equation, $\Delta G^\circ_m = \Delta H^\circ_m - T\Delta S^\circ_m$) are shown in column 6 of Table 3. The ΔS°_m values were all positive and large, supporting the normal expectation of micellization process to be entropy driven.

Table 3. Comparative Thermodynamic Parameters of MEGA-9 in Water at Different Temperatures

	van't Hoff			calorimetry	
T/K	$-\Delta G^\circ_m$/kJ mol^{-1}	$+\Delta H^\circ_m$/kJ mol^{-1}	$+\Delta S^\circ_m$/kJ mol^{-1}	$+\Delta H^\circ_m$/kJ mol^{-1}	$+\Delta S^\circ_m$/kJ mol^{-1}
293	18.6	6.38	85.3	9.32	95.3
298	19.0	5.02	80.7	7.76	89.9
303	19.4	3.69	76.2	5.87	83.4
308	19.8	2.42	72.0	2.64	72.7
313	20.2	1.18	68.2	0.96	67.4
318	20.5	−0.014	64.3	−0.62	62.4
323	20.8	−1.17	60.7	−2.02	58.0

From the calorimetry-determined cmc, ΔH°_m could also be obtained following the van't Hoff rationale (plotting $(\Delta G^\circ_m/T)$ values against $1/T$). Since the plot was nonlinear, a two-degree polynomial equation of the form $(\Delta G^\circ_m/T) = a + b(1/T) + c(1/T)^2$ was used to get ΔH°_m from $[(d(\Delta G^\circ_m/T)]/[d(1/T)] = b + 2c/T = \Delta H^\circ_m$. The ΔH°_m calculated at different temperatures are shown in column 3, Table 3. The two sets of results in columns 3 and 5 differed, although both changed from endo- to exothermic state at temperature ≥318 K. The disagreement of the two types of ΔH°_m for amphiphile aggregation and other processes can be found in the literature.[47,48] Different ΔH°_m by the two procedures may produce different ΔS°_m for the same process; the possibility is more in biological systems where steric factors, group folding–unfolding, ionization, hydrolysis, orientation, etc. may substantially influence the enthalpy and hence the entropy.[48b,c]

In the presence of NaCl and IL, $(\Delta H^\circ_m)_{Cal}$ decreased with increased concentration; even for IL it was exothermic. The two types of ions of IL made unequal contributions; the IL was amphiphilic and NaCl was not. A comparison between the two sets of $(\Delta H^\circ_m)_{vH}$ and $(\Delta H^\circ_m)_{Cal}$ would have been interesting in the presence of NaCl and IL for which more experiments were required. Along with NaCl and IL, calorimetric measurements on the self-association of MEGA-9 were also taken in the presence of 1,4-dioxane (Supporting Information, Figure SM6). This weakly polar aprotic solvent increased cmc by 2-fold at 8 vol % concentration by imparting hydrophobicity in the medium with a dispersing effect on the amphiphile association. Breakdown of water structure delayed the self-association and decreased the process endothermicity more effectively than IL. Scope of solvent effect on the micellization of MEGA-n amphiphiles, therefore, remains quite open.

The values of the standard specific heat of micellization obtained from the slopes of the lines in Figure 3A (i.e., $d\Delta H^\circ_m/dT$) were $(\Delta C^\circ_{p,m})_{vH} = -0.252$ kJ mol^{-1} K^{-1}, and $(\Delta C^\circ_{p,m})_{Cal} = -0.397$ kJ mol^{-1} K^{-1}. The $\Delta C^\circ_{p,m}$ values were related to the number of water molecules involved in the micellization process modeled by Fisicaro et al.[48d] Micelle formation is a hydrophobic process which is better called "hydrophobic association" rather than "hydrophobic bond" formation (since in this process no intermolecular electronic bond is formed). The difference in $\Delta C^\circ_{p,m}$ by calorimetry and van't Hoff method was $\Delta[(\Delta C^\circ_{p,m})_{Cal} - (\Delta C^\circ_{p,m})_{vH}] = -0.145$ kJ mol^{-1} K^{-1} for MEGA-9. For MEGA-10,[23] $(\Delta C^\circ_{p,m})_{vH} \approx (\Delta C^\circ_{p,m})_{Cal}$ with a difference of only −0.05 kJ mol^{-1} K^{-1}. According Fisicaro et al.,[48d] $\Delta C^\circ_{p,m}$ divided by the molar heat capacity of water ($C_{p,w}$ = 75.4 J mol^{-1} K^{-1}) gives the number of water molecules expelled from the solvent to form a cavity to host the amphiphile MEGA-9. These values were herein found to be 3.34 and 5.30 for the van't Hoff and calorimetry methods, respectively (Fisicaro et al.'s value for micelle association falls in the range of 4–19).

The reported ΔS°_m values were positive for both van't Hoff and calorimetry, and they produced nice compensation plots in Figure 3B with compensation temperatures, T^{vH}_{Comp} = 307.4 K and T^{Cal}_{Comp} = 304.6 K; the agreement was good. The T_{Comp} of MEGA-10 by van't Hoff and calorimetry were found to be 311 and 309 K, respectively;[23] their agreement was also good.

ΔG°_m of MEGA-9 like that of MEGA-10[22] can be split in the following way:

dx.doi.org/10.1021/jp400139d | J. Phys. Chem. B XXXX, XXX, XXX–XXX

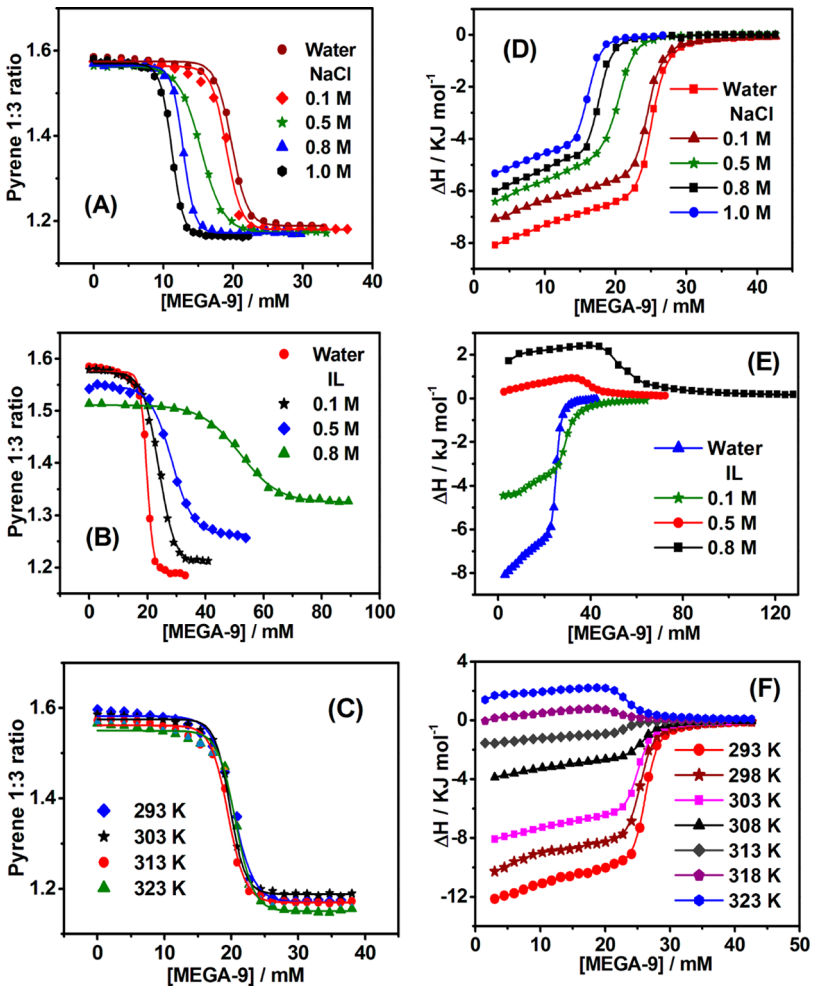

Figure 1. Plots of pyrene 1:3 ratio vs [MEGA-9] (A) in the presence of different [NaCl]; (B) in the presence of different [IL]; (C) at different temperature; and enthalpograms for MEGA-9 dilution in water, (D) in the presence of different [NaCl] (E) in the presence of different [IL]; (F) at different temperature. (In A, B, C the experimental data are fitted to sigmoidal Boltzman equation, and in D, E, F the lines are used to guide the eye only).

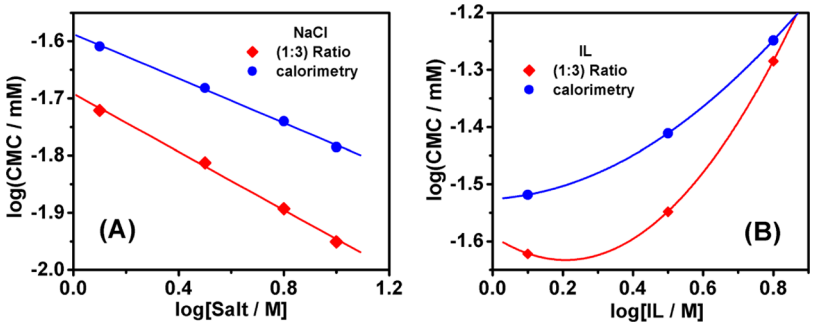

Figure 2. Plots log(cmc) vs concentration of (A) NaCl and (B) IL (with second degree polynomial equation log cmc = $a + b\log(\mathrm{IL/M}) + c\log(\mathrm{IL/M})^2$), where cmc are obtained from both pyrene (1:3) peak ratio and calorimetry.

$$\Delta G^{\circ}_{m} = \Delta G^{\circ}_{m}(\mathrm{HG}) + (n_C - 1)\Delta G^{\circ}_{m}(\mathrm{CH_2}) + \Delta G^{\circ}_{m}(\mathrm{CH_3}) \quad (10)$$

In the relation, HG represents the headgroup of MEGA-9 = $-\mathrm{CH_2CONCH_3CH_2(CHOH)_4CH_2OH}$ and n_C is the number of carbon atoms in the hydrophobic tail (alkyl chain) of the surfactant which is 7. $\Delta G^{\circ}_{m}(\mathrm{CH_2})$ and $\Delta G^{\circ}_{m}(\mathrm{CH_3})$ can be taken to be[22] −2.92 and −8.78 kJ mol^{-1}, respectively. These values were used in the ΔG°_{m} relation (eq 12) to calculate $\Delta G^{\circ}_{m}(\mathrm{HG})$ at different temperatures. Their temperature dependence then was considered in the van't Hoff relation to get $\Delta G^{\circ}_{m}(\mathrm{CH_2})$ and $\Delta H^{\circ}_{m}(\mathrm{CH_3})$, and the corresponding $\Delta S^{\circ}_{m}(\mathrm{CH_2})$ and $\Delta S^{\circ}_{m}(\mathrm{CH_3})$. The evaluated $\Delta G^{\circ}_{m}(\mathrm{HG})$ values in the temperature range of 293−323 K varied between 7.7 and 5.5 kJ mol^{-1}. $\Delta H^{\circ}_{m}(\mathrm{HG})$ and $\Delta S^{\circ}_{m}(\mathrm{HG})$ were found to be 32.2 kJ mol^{-1} and 83.6 J mol^{-1} K^{-1}, respectively at 298 K.

The ΔG°_{m} found from the eq 9 does not contain contribution from the micelle aggregation number. Relations

dx.doi.org/10.1021/jp400139d | J. Phys. Chem. B XXXX, XXX, XXX−XXX

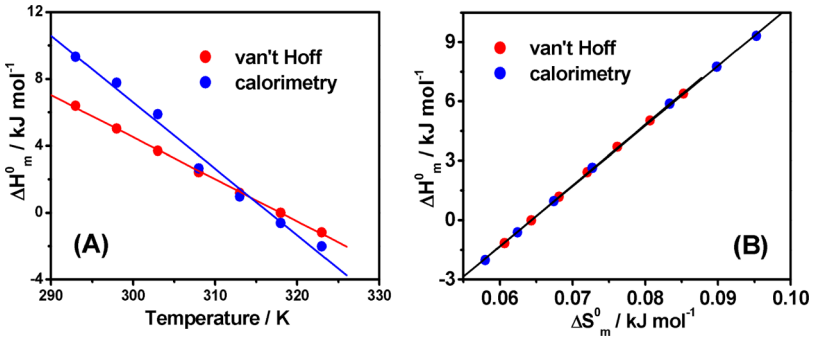

Figure 3. (A) Dependence of ΔH°_{m} on temperature for micellization of MEGA-9 by van't Hoff and calorimetry methods. (B) Enthalpy−entropy compensation plots for the micellization of MEGA-9 by van't Hoff and calorimetry methods.

containing contributions of N on ΔG°_{m} are available in the literature but are rarely used for a comparison. We did it in the past for the micellization of MEGA-10[23] which is also done herein. Corkill's[49] and Moroi's[50] relations (shown below) were used for this purpose.

Corkill relation:

$$\Delta G^{\circ}_{m}(\mathrm{II}) = \left(1 - \frac{1}{N}\right)RT \ln X_{cmc} + \frac{RT}{N}\left[\ln\left\{\frac{N^2(2N-1)}{N-2}\right\} + (N-1)\ln\left\{\frac{N(2N-1)}{2(N^2-1)}\right\}\right] \quad (11)$$

Moroi relation:

$$\Delta G^{\circ}_{m}(\mathrm{III}) = RT \ln X_{cmc} + \frac{RT}{N}[\ln 2 + 2 \ln N] \quad (12)$$

The results are compared in Table 4. There results of an earlier study[23] on MEGA-10 are shown in the parentheses. The

Table 4. Comparison of ΔG°_{m} at 303 K Using Different Relations 9, 11, and 12[a]

T/K	N	$-\Delta G^{\circ}_{m}$(I)/kJ mol^{-1}	$-\Delta G^{\circ}_{m}$(II)/kJ mol^{-1}	$-\Delta G^{\circ}_{m}$(III)/kJ mol^{-1}
293	83	18.6 (22.0)	18.1 (21.3)	18.3 (20.6)
303	87	19.4 (22.9)	18.9 (22.3)	19.1 (21.5)
313	80	20.2 (23.7)	19.7 (22.9)	20.1 (22.0)
323	84	20.8 (24.4)	20.3 (24.0)	20.5 (23.2)

[a]The relations (9), (11), and (12) are used as per the Results and Discussion section.

differences of ΔG°_{m}(II) and ΔG°_{m}(III) from ΔG°_{m}(I) mean the contributions of N in the evaluation. They showed the trend ΔG°_{m}(I) < ΔG°_{m}(III) < ΔG°_{m}(II). The consideration of the contribution of N in the free energy term made it higher than without. The differences were minor; such differences for MEGA-10 micellization were higher than MEGA-9. It is evident from eqs 13 and 14 that higher N values would decrease its contribution to ΔG°_{m}; for N > 100 the effect can be neglected; eq 9 is then applicable.

Kresheck has proposed a relationship between $\Delta C^{\circ}_{p,m}$ and water-accessible surface area (ASA) of nonpolar groups of the nonionic surfactants.[51a,b] Values of ASA could be a measure of the extent of hydration of the micelle interior or the number of the buried carbon atoms in the penetrated water in the micelle. Thus

$$\mathrm{ASA}_{exp} = \frac{\Delta C^{\circ}_{p,m}}{-1.463} \quad (13)$$

For MEGA-9, $\Delta C^{\circ}_{p,m}$ by van't Hoff and ITC methods were found to be −0.252 and −0.397 kJ mol^{-1} K^{-1}, respectively; the corresponding ASA_{exp} values by eq 13 were 172.2 and 271.4 Å^2. The ASA_{exp} and n (buried carbon number) presented in Table 3 of Kresheck's paper[51b] followed a linear correlation, ASA_{exp} = 83.6 + 29.3n (plot not shown). Using our ASA_{exp} values in the linear relation, the n values were found to be 3 and 6 for MEGA-9 micelles corresponding to van't Hoff and ITC results, respectively. Thus, water penetration in the micelle was either up to 3 or 6 carbon atoms. By NMR studies[51c−e] it has been shown that surfactant micelles containing polyethylene hydrophobic chains allow water penetration to a fair length even up to 7 carbon atoms.[51d] Kresheck's proposition is thus on the right track; our value of n = 6 on MEGA-9 micelles from calorimetry was on the higher side.

3.4. Microenvironment Properties of MEGA-9 Micelles. Microenvironment of MEGA-9 micelles was examined by using two probes coumarin-153 (C-153) and ANS. The fluorophore C-153 was a hydrophobic probe, whereas ANS was a dual (hydrophilic−hydrophobic) probe. The former could give information only on the nonpolar region of the micelle whereas ANS offered information on the interfacial polar−apolar region where it essentially resided in a distributed form.[52,53] Both steady-state and time-resolved fluorescence measurements were taken to get the probes' characteristics in the region of their residence. The results are discussed below.

3.4.1. Steady-State Fluorescence Study. Fluorescence emission spectra of ANS and C-153 in micellar solution of MEGA-9 in NaCl, IL and at different temperatures could lend a first-hand knowledge on the microenvironment of the probe in the micellar phase.[54−56] Such spectra are presented in Figure 4A−F. The emission peak of ANS at 303 K was at 489 nm in aqueous micellar solution of MEGA-9 like that of MEGA-10.[19] For C-153 the emission peak at room temperature was at 450 nm in the nonpolar n-heptane medium,[57,58] and 548 nm in water.[39b] In MEGA-9 micellar medium the emission peak was at 529 nm. It indicated that C-153 in the MEGA-9 micellar solution remained in a region where the polarity was lower than that of water but reasonably higher than n-heptane, suggesting that the probe probably resided in a layer fairly below the micelle−water interface. Water penetration in the micelle interior discussed in section 3.3 is further supported. Figure 4A−C shows the emission spectra of ANS (λ_{max} = 489 nm) in

dx.doi.org/10.1021/jp400139d | J. Phys. Chem. B XXXX, XXX, XXX−XXX

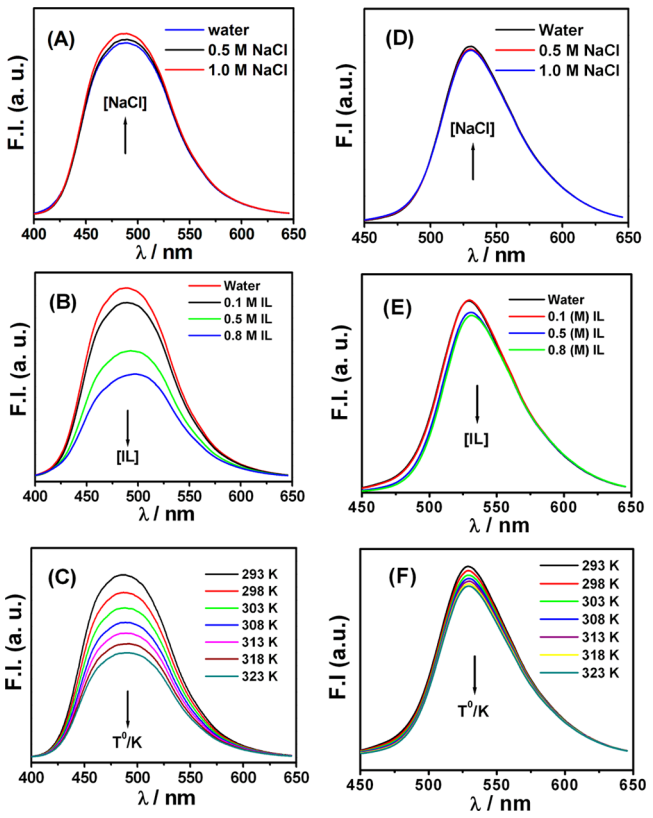

Figure 4. Steady-state emission spectra of ANS, (A) at different [NaCl]; (B) at different [IL]; (C) at different temperatures and emission spectra of C-153, (D) at different [NaCl]; (E) at different [IL]; (F) at different temperatures.

the presence of NaCl and IL and at different temperatures, respectively. In the case of NaCl, fluorescence intensity enhanced to a small extent, indicating less polar environment sensed by the probe. In the case of IL, the probe sensed more polar environment with 8 nm (489−497 nm) red shift at higher [IL], and temperature decreased the emission; the probe continued to reside in the higher hydrophilic environment. In the case of C-153, shown in Figure 4D−F, the emission (having λ_{max} = 529 nm) was hardly affected by NaCl up to 1 M; the local environment remained unaltered. In the presence of 0.8 M IL, there was only a modest decrease in the emission intensity with λ_{max} = 531 nm (a small red shift). The local polarity of the probe increased to some extent. The temperature dependence of the emission spectra of C-153 in MEGA-9 micelle was similar to the effect of IL. The absorption spectra of the probes in the presence of additives remained almost unchanged. The enhanced solvent sensitivity of fluorescence than absorbance was caused by the increased solute (probe)−solvent interaction in the excited state by way of increased dipole moment upon excitation.

The pyrene 1:3 emission peak intensity ratio index is also a well-known parameter that provides information on the local polarity and the solubilization site of the probe in the organized media.[53] Post-micellar 1:3 ratio index remained almost independent of the presence of NaCl and temperature. Thus, the cybotactic section of pyrene remained almost unaffected by the influence of both NaCl and temperature. But in the case of IL the results were different. It is well established that, on the average, pyrene locates itself in the palisade layer of the micellar pseudophase,[53b,59] so the increase of 1:3 ratio clearly indicated that the cybotactic section was modified by the addition of IL; IL made it more polar. There were two possibilities: (a) introduction of IL into the solution caused entry of solvated water molecules through its headgroup into the micelle enhancing its overall solvation, and (b) the increased surface area per headgroup of the polar IL forced the probe to be located to the outer peripherial region. On the whole, addition of IL induced formation of micelles with open (or loose) structure, favoring penetration of solvent or solvation.

Microviscosity of the solubilization site of the probe in its environment obtained from the steady-state fluorescence anisotropy measurements[31] would give information on the motion of the probe molecule in its site of residence in the

Table 5. Steady-State Fluorescence Anisotropy and Decay Parameters of ANS in 200 mM MEGA-9 Micelles with Various Concentrations of Additives at 303 K and in Pure Water at Different Temperatures

Section A								
additives	concn (M)	r_{ss}[a]	α_1	τ_1 (ns)	α_2	τ_2 (ns)	$\langle\tau\rangle$ (ns)[b]	χ^2
NaCl	0	0.071 ± 0.001	0.49	2.73	0.51	3.99	3.49	1.00
	0.1	0.073 ± 0.002	–	–	–	–	–	–
	0.5	0.077 ± 0.001	0.52	2.79	0.48	4.13	3.56	0.99
	0.8	0.080 ± 0.003	–	–	–	–	–	–
	1.0	0.082 ± 0.001	0.48	2.83	0.52	4.21	3.67	1.12
[bmim][BF_4]	0.1	0.069 ± 0.001	–	–	–	–	–	–
	0.5	0.062 ± 0.002	0.65	2.31	0.35	3.50	2.84	1.05
	0.8	0.054 ± 0.001	0.69	2.05	0.31	3.49	2.67	1.04
Section B								
medium	T/K	r_{ss}[a]	α_1	τ_1 (ns)	α_2	τ_2 (ns)	$\langle\tau\rangle$ (ns)[b]	χ^2
water	293	0.090 ± 0.001	0.36	2.63	0.64	4.36	3.92	1.01
	298	0.080 ± 0.001	–	–	–	–	–	–
	303	0.071 ± 0.003	0.49	2.73	0.51	3.99	3.49	1.00
	308	0.062 ± 0.002	–	–	–	–	–	–
	313	0.053 ± 0.001	0.75	2.81	0.25	3.86	3.14	1.01
	318	0.048 ± 0.002	–	–	–	–	–	–
	323	0.044 ± 0.001	0.76	2.58	0.24	3.36	2.81	0.99

[a]Mean value ± standard deviation of five measurements. [b]Mean value of three individual measurements.

dx.doi.org/10.1021/jp400139d | J. Phys. Chem. B XXXX, XXX, XXX−XXX

micelles.[31,60,61] Table 5 shows two opposite effects on steady-state anisotropy of ANS on addition of NaCl and IL in micellar medium at a fixed temperature. The temperature had identical but increased effect compared to IL. ANS sensed less interfacial rigid environment with increase of temperature. For C-153, the rigidity of the micelle environment around the probe remained almost invariant with [NaCl]; both IL and temperature sensed similar kind of rigid microenvironment. Depolarization of the light from the probe associated with micelles produced different rotational processes including movement of the probe in the micelle and the rotation of the micelle itself.[31]

3.4.2. Time-Resolved Fluoresence Study. The lifetime of the probe is a sensitive indicator of the local environment in which the probe molecule is solubilized in the complex environment. The ANS has shown a biexponential decay profile (Figure 5A)

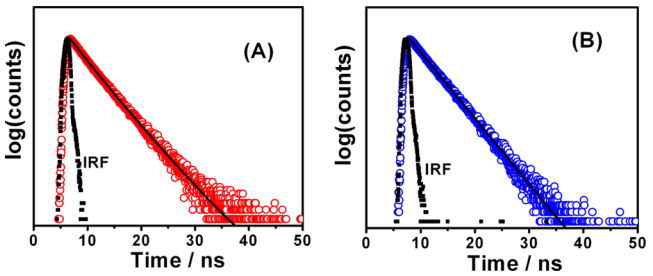

Figure 5. Representative fluorescence decays of (A) ANS in MEGA-9 micelles in pure water and (B) C-153 in MEGA-9 micelles at 303 K temperature. The solid lines are best fit through the data points. IRF is the instrumental response function.

of its fluorescence in MEGA-9 micelles at 303 K similar to the reports of Hierrezuelo et al.[19] on MEGA-10. The biexponential fitting did not necessarily mean that the decay curve has only two discrete time constants. It implied distribution of time constants around two well-separated values, suggesting distribution of the probe between two regions in the interface: the top polar region and the nonpolar lower palisade region. The distribution remained virtually independent of NaCl concentration (Table 5, section A), and the average ratio of its fraction in the polar and nonpolar regions α_1 and α_2, respectively, was 1:1, and τ_1 (fast decay component) and τ_2 (slow decay component) increased with [NaCl]. In the presence of IL, both τ_1 and τ_2 declined, and the distribution of the probe between the two regions altered ($\alpha_1 > \alpha_2$). More penetration of water into the first region was supported (τ_1 decreased more than τ_2). The average decay time $\langle\tau\rangle$ (obtained from eq 5) also supported the above rationale. The temperature effect on the time-resolved decay of ANS emission behaved like that with IL (Table 5, section B). In the time-resolved measurements, C-153 emission showed a single-exponential decay function (Figure 5B). Similar behavior of C-153 in OTG micelles was reported.[64] Lifetime of the probe remained virtually unaltered in the presence of NaCl (Table 6, section A), indicating its stability in the environment. In IL medium the lifetime decreased with increasing concentration, and the effect of temperature was also like the IL (Table 6, section B). The results corroborated the steady-state findings.

The time-dependent fluorescence anisotropy is a sensitive indicator of the rotational motion and/or rotation-relaxation of the fluorophore in an organized assembly.[31,55,56,60,61] The time-resolved decay of polarization anisotropy $r(t)$ was calculated from the fluorescence decays in parallel and perpendicular

Table 6. Steady-State Fluorescence Anisotropy and Decay Parameters of C-153 in 200 mM MEGA-9 Micelles with Various Concentrations of Additives at 303 K

Section A				
additives	concn	r_{ss} [a]	τ (ns)[b]	χ^2
NaCl	0	0.066 ± 0.001	3.50	1.06
	0.1	0.065 ± 0.002	3.50	1.02
	0.5	0.067 ± 0.001	3.44	1.06
	0.8	0.069 ± 0.002	3.43	1.08
	1.0	0.071 ± 0.001	3.46	1.11
[bmim][BF_4]	0.1	0.063 ± 0.001	3.48	1.05
	0.5	0.055 ± 0.001	3.41	1.01
	0.8	0.049 ± 0.001	3.37	1.09
Section B				
medium	T/K	r_{ss} [a]	τ (ns)[b]	χ^2
water	293	0.084 ± 0.001	3.55	1.05
	298	0.072 ± 0.002	–	–
	303	0.066 ± 0.001	3.50	1.06
	308	0.051 ± 0.001	–	–
	313	0.047 ± 0.001	3.48	1.04
	318	0.038 ± 0.002	–	–
	323	0.033 ± 0.002	3.45	1.02

[a]Mean value ± standard deviation of five measurements. [b]Mean value of three individual determinations.

directions with respect to the excitation polarization as follows:[31]

$$r(t) = \frac{I_{VV}(t) - GI_{VH}(t)}{I_{VV}(t) + 2GI_{VH}(t)} \quad (14)$$

where G is a correction factor for detector sensitivity to the polarization direction of emission, t is the time, and the subscripts VV and VH denote vertical excitation, and vertical and horizontal emission polarizations, respectively.[62] The orientation time correlation function is described by the relation[63,64]

$$r(t) = \sum_i r_i \exp(-t/\tau_{i,r}) \quad (15)$$

where r_i and $\tau_{i,r}$ are the individual amplitude and reorientation time constant for the ith anisotropy decay, respectively.

The fluorescence depolarization anisotropies ($r(t)$) of C-153 and ANS in MEGA-9 micelles were obtained (from eq 14) with best fit to the single exponential (eq 15). A representative profile of anisotropy decay is displayed in Figure 6A,B, and the relevant dynamic parameters are tabulated in Table 7. In all the studied environments, the reorientation time constant was

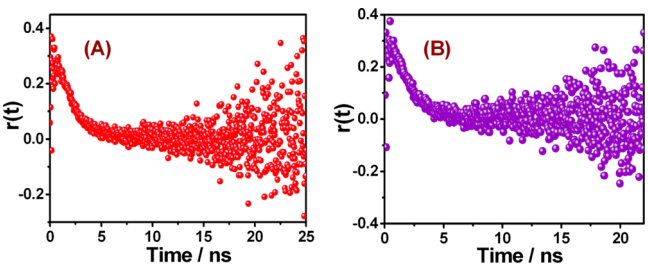

Figure 6. Representative time-resolved fluorescence anisotropy decay profile of (A) ANS and (B) C-153 in aqueous solution of MEGA-9 at 303 K temperature.

dx.doi.org/10.1021/jp400139d | J. Phys. Chem. B XXXX, XXX, XXX–XXX

Table 7. Reorientation−Dynamical Parameters of C-153 and ANS in MEGA-9 Micelles with Various Concentrations of Additives at 303 K and in Pure Water at Different Temperatures

Section A								
		C-153			ANS			
additives	concn (M)	r_0	τ_r (ns)	χ^2	r_0	τ_r (ns)	χ^2	τ_m (ns)
NaCl	0	0.36	1.77	1.07	0.43	1.88	1.13	15.5
	0.1	–	–	–	–	–	–	–
	0.5	0.37	1.86	1.06	0.41	1.92	1.16	17.3
	0.8	–	–	–	–	–	–	–
	1.0	0.35	1.85	0.99	0.42	2.01	1.15	29.2
[bmim][BF_4]	0.1	–	–	–	–	–	–	–
	0.5	0.39	1.69	1.23	0.39	1.55	1.16	22.1
	0.8	0.38	1.63	1.26	0.40	1.39	1.13	20.7

Section B								
		C-153			ANS			
medium	T/K	r_0	τ_r (ns)	χ^2	r_0	τ_r (ns)	χ^2	τ_m (ns)
water	293	0.39	2.25	1.05	0.40	2.27	1.11	15.5
	298	–	–	–	–	–	–	–
	303	0.36	1.77	1.07	0.43	1.88	1.15	11.4
	308	–	–	–	–	–	–	–
	313	0.39	1.51	1.02	0.39	1.51	1.18	7.80
	318	–	–	–	–	–	–	–
	323	0.38	1.25	1.00	0.41	1.20	1.16	5.42

faster than the corresponding fluorescence lifetime in the same environment, revealing that the excited-state fluorescence depolarization of the probes essentially completed within the excited-state lifetime. Moreover, the decrease in the reorientation time constant of C-153 and ANS with increase of temperature as well as with addition of IL possibly arose by way of increased mechanically trapped water molecules in the MEGA-9 micelles. The faster response of these water molecules than the bound water molecules led to a faster rotation-relaxation dynamics in the micelles. Several reasons may be considered to account for the reorientation of the fluorescence anisotropy of the micelle bound probe; they are the following:[39b,54−56]

(i) The fluorophore rotates within the micelle; (ii) the entrapped fluorophore cannot rotate but the micelle unit carrying the probe rotates; and (iii) both rotations are operative. The third option is neglected for the anisotropy decay was single-exponential. To confirm one of the former two possibilities, we have calculated the rotational-relaxation times of the micellar units (τ_m) according to the Stokes−Einstein−Debye (SED) relation.

$$\tau_m = \frac{4\pi R_h^3 \eta}{3k_B T} \tag{16}$$

where R_h is the hydrodynamic radius of the micellar units (obtained from DLS measurements and summarized in Tables 1 and 2), η is the viscosity of the medium, k_B is the Boltzmann constant, and T is the temperature in kelvin. The τ_m values are shown in Table 7, column 5. They were all much higher than τ_r in the studied environments, supporting that the observed reorientation dynamics were attributable to the rotational motion of the probe only and not of the micelles.[61]

The temperature dependence of the decay constant τ_2 of ANS and τ of C-153 were the measures of viscosity of the micelle regions they probed. Similarly, the rotational constant (τ_r) of C-153 and ANS in the micelle was also a measure of viscosity of the regions of their residence. An equation[65] of the following form was considered applicable

$$\frac{1}{\tau_v} = \left(\frac{k_B T}{h}\right) \exp(\Delta S_a/R) \exp(-E_a/RT) \tag{17}$$

or

$$\ln\left(\frac{1}{\tau_v}\right) = \ln\left(\frac{k_B}{h}\right) + \ln T + \frac{\Delta S_a}{R} - \frac{E_a}{RT} \tag{18}$$

where τ_v stands for τ_2 or τ or τ_r and E_a and ΔS_a are the corresponding activation energy and entropy of activation, respectively, and h is the Planck constant.

The plots of $\ln(1/\tau_2)$ versus $1/T$, $\ln(1/\tau)$ versus $1/T$, and $\ln(1/\tau_r)$ versus $1/T$ were excellently linear according to transition state theory neglecting $\ln T$ (being small) (Figure SM7 in the Supporting Information). Their slopes and intercepts were used to get the activation energy and entropy of activation, respectively. The C-153 − MEGA-9 system produced 0.72 kJ mol^{-1} and −205.5 J mol^{-1} K^{-1} as energy of activation $(E_a)_\tau$ and entropy of activation $(\Delta S_a)_\tau$, respectively. The corresponding results for ANS-MEGA-9 system were $(E_a)_{\tau 2}$ = 6.4 kJ mol^{-1} and $(\Delta S_a)_{\tau 2}$ = −187.9 J mol^{-1} K^{-1}, respectively. In the MEGA-9 micelle system, the probe C-153 experienced 9-fold less energy barrier than ANS. The entropy of activation was, on the other hand, comparable. The structure of the transition state was ordered. The rotational constant of C-153 in MEGA-9 micelles was associated with $(E_a)_{\tau r}$ = 15.1 kJ mol^{-1} and $(\Delta S_a)_{\tau r}$ = −152.4 J mol^{-1} K^{-1}, whereas those for ANS were $(E_a)_{\tau r}$ = 16.0 kJ mol^{-1} and $(\Delta S_a)_{\tau r}$ = −147.3 J mol^{-1} K^{-1}. The difference between the two E_a was minor; although their regions of residence were different. Solvent penetration and removal in the regions made the overall morphology state energetically comparable. The ΔS_a produced a small component of difference of 5.1 J mol^{-1} K^{-1} between C-153 and ANS by way of a small difference (0.9 kJ mol^{-1}) in E_a.

dx.doi.org/10.1021/jp400139d | J. Phys. Chem. B XXXX, XXX, XXX−XXX

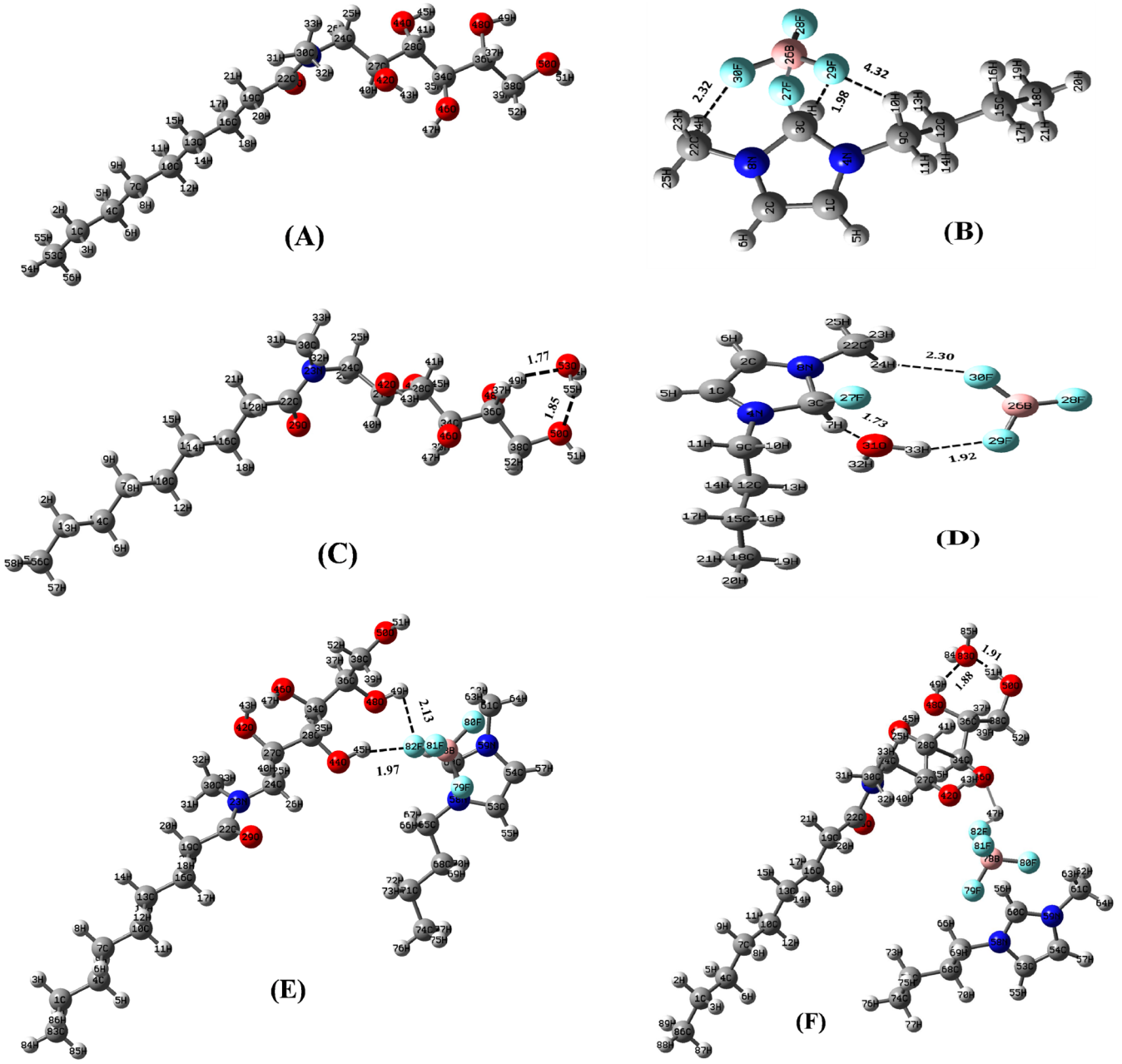

Figure 7. B3LYP/6-31G(d,p)-optimized structure: (A) MEGA-9, (B) IL, (C) MEGA-9/H_2O complex, (D) IL/H_2O complex, (E) MEGA-9/IL complex, and (F) MEGA-9/IL/H_2O complex. Color code for atoms: Blue, nitrogen; red, oxygen; dark gray, carbon; light gray, hydrogen; sea green, boron; and aqua green, fluoride ion.

3.5. DFT Calculations. Interaction of amphiphilic bodies with solvent and additives can be qualitatively understood through density functional theory (DFT) calculation. For such an understanding of the interactions of MEGA-9 with IL and H_2O, we have performed model calculations using B3LYP[66a,b] functional with the standard basis set, 6-31G(d,p), for all atoms. All the structures correspond to true minima of the potential energy surface confirmed by the vibrational frequency calculations and total simulations performed using Gaussian 03 program.[66b] We first optimized the structures of the isolated MEGA-9, IL, and H_2O, the (1:1) binary complexes of MEGA-9 with IL and H_2O, and the (1:1:1) ternary complex of MEGA-9, IL, and H_2O. The most stable optimized structures are presented in Figure 7, and their interaction energies (the energy difference between complexes and the monomers) are listed in Table 8. We did not make the basis set superposition error (BSSE) correction since we were interested only in relative interaction strength and validity of this correction has been recently questioned.[67] The present results showed a highly stable MEGA-9/IL/H_2O trimer complex with the

Table 8. Interaction Energies (E_{int}) of the Complexes between MEGA-9, H_2O, and IL

complex system	interaction energy ($-E_{int}$/kcal mol^{-1})
IL + H_2O	21.87
MEGA-9 + H_2O	12.92
MEGA-9 + IL	80.93
MEGA-9 + IL + H_2O	133.31

dx.doi.org/10.1021/jp400139d | J. Phys. Chem. B XXXX, XXX, XXX−XXX

binding energy of 133.31 kcal mol^{-1} shown in the table. Strong interaction with IL caused a large increase in cmc of MEGA-9. The order of stability of the proposed complexes were MEGA-9/H_2O < IL/H_2O < MEGA-9/IL < MEGA-9/IL/H_2O. We were also interested in the cooperativity of the molecular trimer containing X, Y, and Z molecules given by the three-body term E_{3B},[68] which is defined as the difference between the total interaction energy E_{int} and the sum of the pairwise or two-body interaction energies E_{2B}:

$$E_{3B} = E_{int}(XYZ) - E_{2B}(XY) - E_{2B}(YZ) - E_{2B}(XZ) \quad (19)$$

Here, $E_{int}(XYZ)$ is the energy of the trimer relative to three monomers in the complex geometry, neglecting any one-body or deformation energies,[69] which are small in these complexes. If E_{3B} is positive, an anticooperative interaction of the three-monomer units is diagnosed; i.e., the sum of all pair interaction energies is more favorable than the total interaction energy. The calculated value of E_{3B} = −17.6 kcal mol^{-1} which is 13.2% of $E_{int}(XYZ)$. The three-body interaction (MEGA-9/IL/H_2O) was thus cooperative; the pairwise interactions of (MEGA-9/IL, MEGA-9/H_2O, and IL/H_2O) were more favorable than the total interaction energy. Similar was the finding of Weimann et al.[68a] on the HCl/methanol system, and that of Das et al.[68c] on the Aerosol OT/ethylene glycol/water system.

4. CONCLUSION

Although salts show weak effect on the micellization of nonionic surfactants, the influences of NaCl and the ionic liquid (imidazolium tetrafluoroborate) on MEGA-9 were appreciable. NaCl decreased cmc by the salting out effect, whereas IL increased it by way of introducing nonpolarity in solution due to its butylmethyl cation in solution (a salting in type effect). The dependence of micellar parameters on [NaCl] was different (mostly opposite) to that on [IL]; nevertheless, the energetic parameters showed parity but their magnitudes were unequal. The ΔH°_m obtained from the van't Hoff method and from calorimetry were noncomparable; ΔH°_m by calorimetry was lower than that by van't Hoff. The integral method of calorimetry recorded heats absorbed or released from all possible physical-chemical processes operative in the system whereas the differential process of van't Hoff estimated only the micelle formation process (hence the difference). Therefore, thermodynamic evaluation of a process by determining enthalpy by calorimetry has to be considered with reservation. Nevertheless, for understanding the contributions from other related or involved processes evaluation by both the methods are required. In the calculation of ΔG°_m(I) by eq 9, contribution of N was neglected (which is the normal practice). Using the measured N, calculation of ΔG°_m(II) and ΔG°_m(III) by Corkil and Moroi equations were done; they were modestly different. Estimate of ASA_{exp} from the $\Delta C^\circ_{p,m}$ suggested water penetration into the MEGA-9 micelle to the extent of 3−6 carbon atoms, which fairly corroborated by the existing knowledge from other studies. Steady-state fluorescence measurements and the pyrene 1:3 florescence peak ratio index supported water penetration in MEGA-9 micelle interior.

Gross shape of the MEGA-9 micelles was spherical that to some extent increased with NaCl addition together with N by a salting out effect. IL addition produced a reverse effect on N; decreased size by decreased N was compensated for by solvent penetration in the loose assembly structure of MEGA-9 by the salting in effect of IL.

Static fluorescent emission supported unchanged micelle property in the presence of NaCl, whereas both IL and temperature produced increased polarity. The hydrophilic and hydrophobic ANS evenly distributed between the polar and nonpolar regions of the MEGA-9 micelles to manifest biexponential fluorescence decay curves in the time-resolved measurements. NaCl did not affect the distribution, while both IL and temperature affected it, the interfacial layer became more polar. For C-153, the fluorescence emission curves were monoexponential, and the palisade layer of its residence was hardly affected by NaCl and slightly affected by IL but the effect of temperature was more (r_{ss} fairly decreased but the τ decreased slightly). The decay of fluorescence depolarization was single exponential for ANS and C-153, and rotation of the probe in the micelle was faster than that of the micelle itself. In aqueous medium, dynamics of the fluorescence decay and rotation of the probe in the micelle produced larger energy barrier for the fluorescence decay for both ANS and C-153. The residency of the solvated probe ANS in the polar region was accounted for its greater barrier than C-153 that remained in the palisade region. The rotational freedoms of both were close to yield comparable $(E_a)_{rr}$. The activation entropy difference of the former (1.4 eu) was more compared to the latter (5 eu).

DFT calculation has found maximum stability in the MEGA-9/IL/H_2O combination than the binary combinations MEGA-9/H_2O, IL/H_2O, and MEGA-9/IL. Also, the stabilization energy of MEGA-9/IL was the second highest among them all. This explained the large effect of hindrance of IL to the micellization of MEGA-9.

■ ASSOCIATED CONTENT

Ⓢ Supporting Information

Profiles of determination of cmc and enthalpy of micellization (ΔH°_m) from ITC and tensiometry; plots for the determination of aggregation number (N) of MEGA-9 micelle; DLS plots for the determination of hydrodynamic radius (R_h); and plots for evaluation of energy of activation (E_a) and entropy of activation (ΔS_a) of the probes ANS and C-153 in MEGA-9 micellar medium. This material is available free of charge via the Internet at http://pubs.acs.org.

■ AUTHOR INFORMATION

Corresponding Author

*Phone: +91-33-2414-6411. Fax: +91-33-2414-6266. E-mail: spmcss@yahoo.com.

Notes

The authors declare no competing financial interest.

■ ACKNOWLEDGMENTS

A.P., S.M., and B.N. are thankful to UGC, Government of India, New Delhi, for granting Senior Research Fellowship. S.P.M. thanks Jadavpur University and Indian National Science Academy for the positions of Emeritus Professor and Honorary Scientist, respectively. Financial assistance from DST is acknowledged.

■ REFERENCES

(1) He, Y. Y.; Li, Z. B.; Simone, P.; Lodge, T. P. Self-Assembly of Block Copolymer Micelles in Ionic Liquid. *J. Am. Chem. Soc.* **2001**, *128*, 2745−2750.

(2) Alexandridis, P., Lindman, B., Eds.; *Amphiphilic Block Copolymers: Self-Assembly and Applications*; Elsevier: Amsterdam, 2000.

(3) Jaramillo, T. F.; Baeck, S. H.; Cuenya, B. R.; McFarland, E. W. Catalytic Activity of Supported Au Nanoparticles Deposited from Block Copolymer Micelles. *J. Am. Chem. Soc.* **2003**, *125*, 7148−7149.
(4) Allen, C.; Maysinger, D.; Eisenberg, A. Nano-Engineering Block Copolymer Aggregates for Drug Delivery. *Colloids Surf. B* **1999**, *16*, 3−27.
(5) Kang, W.; Liu, Y.; Qi, B.; Liao, G.; Yang, Z.; Hong, J. Interactions Between Alkali/Surfactant/Polymer and Their Effects on Emulsion Stability. *Colloids Surf. A* **2000**, *175*, 243−247.
(6) (a) Moulik, S. P.; Paul, B. K. Structure, Dynamic and Transport Properties of Microemulsions. *Adv. Colloid Interface Sci.* **1998**, *78*, 99−195. (b) Zhang, J.; Li, L.; Wang, J.; Sun, H.; Xu, J.; Sun, D. Double Inversion of Emulsions Induced by Salt Concentration. *Langmuir* **2012**, *28*, 6769−6775.
(7) Uchegbu, I. F.; Vyas, S. P. Non-ionic Surfactant Based Vesicles (niosomes) in Drug Delivery. *Int. J. Pharm.* **1998**, *172*, 33−70.
(8) Šegota, S.; Težak, D. Spontaneous Formation of Vesicles. *Adv. Colloid Interface Sci.* **2006**, *121*, 51−75.
(9) Hao, J. C.; Song, A. X.; Wang, J. Z.; Chen, X.; Zhuang, W. C.; Shi, F.; Zhou, F.; Liu, W. Self-Assembled Structure in Room-Temperature Ionic Liquids. *Chem.—Eur. J.* **2005**, *11*, 3936−3940.
(10) (a) Evans, D. F.; Miller, D. D. In *Organized Solutions. Surfactants in Science and Technology*; Friberg, S. E.; Lindman, B., Eds.; Dekker: New York, 1992. (b) Fendler, J. H. *Membrane Mimetic Chemistry: Chracterizations and Applications of Micelles, Microemulsions, Monolayers, Bilayers, Vesicles and Host-Guest Systems*; Wiley: New York, 1983.
(11) Rosen, M. J. *Surfactants and Interfacial Phenomena*, 2nd ed.; Wiley: New York, 1989.
(12) (a) Molina-Bolívar, J. A.; Aguiar, J.; Peula-García, J. M.; Ruiz, C. C. Surface Activity, Micelle Formation, and Growth of N-Octyl-B-D-Thioglucopyranoside in Aqueous Solutions at Different Temperatures. *J. Phys. Chem. B* **2004**, *108*, 12813−12820. (b) Rodriguez, A.; Graciani, M.; del, M.; Moya, M. L. Effect of Addition of Polar Organic Solvents on Micellization. *Langmuir* **2008**, *24*, 12785−12792. and references therein. (c) Rodriguez, A.; Graciani, M.; del, M.; Angulo, M.; Moya, M. L. Effects of Organic Solvent Addition on The Aggregation and Micellar Growth of Cationic Dimeric Surfactant 12−3-12, $2Br^-$. *Langmuir* **2007**, *23*, 11496−11505. (d) Zana, R.; Yiv, S.; Strazielle, C.; Lianos, P. Effect of Alcohol on The Properties of Micellar Systems: I. Critical Micellization Concentration, Micelle Molecular Weight and Ionization Degree, and Solubility of Alcohols in Micellar Solutions. *J. Colloid Interface Sci.* **1981**, *80*, 208−223. (e) Zana, R. Aqueous Surfactant-Alcohol Systems: A Review. *Adv. Colloid Interface Sci.* **1995**, *57*, 1−64 and references therein..
(13) (a) Pan, A.; Naskar, B.; Prameela, G. K. S.; Phani Kumar, B. V. N.; Mandal, A. B.; Bhattacharya, S. C.; Moulik, S. P. Amphiphile Behavior in Mixed Solvent Media I: Self-Aggregation and Ion Association of Sodium Dodecyl Sulfate in 1,4-Dioxane-Water and Methanol-Water Media. *Langmuir* **2012**, *28*, 13830−13843. (b) Naskar, B.; Dan, A.; Ghosh, S.; Aswal, V. K.; Moulik, S. P. Revisiting the Self-Aggregation Behavior of Cetyltrimethylammonium Bromide in Aqueous Sodium Salt Solution with Varied Anions. *J. Mol. Liq.* **2012**, *170*, 1−10.
(14) Boullanger, P.; Chevalier, Y. Surface Active Properties and Micellar Aggregation of Alkyl 2-Amino-2-Deoxy-B-D-Glucopyranosides. *Langmuir* **1996**, *12*, 1771−1776.
(15) Shinoda, K.; Carlsson, A.; Lindman, B. On the Importance of Hydroxyl Groups in the Polar Head-Group of Nonionic Surfactants and Membrane Lipids. *Adv. Colloid Interface Sci.* **1996**, *64*, 253−271.
(16) Söderman, O.; Johänsson, I. Polyhydroxyl-Based Surfactants and their Physico-Chemical Properties and Applications. *Curr. Opin. Colloid Interface Sci.* **2000**, *4*, 391−401.
(17) Briganti, G.; Puvvada, S.; Blankschtein, D. Effect of Urea on Micellar Properties of Aqueous Solution of Nonionic Surfactant. *J. Phys. Chem.* **1991**, *95*, 8989−8995 and references therein..
(18) Ruiz, C. C.; Sanchez, G. F. Effect of Urea on Aggregation Behavior of Triton X-100 Micellar Solutions: A Photophysical Study. *J. Colloid Interface Sci.* **1994**, *165*, 110−115.
(19) Hierrezuelo, J. M.; Molina-Bolívar, J. A.; Ruiz, C. C. On the Urea Action Mechanism: A Comparative Study on the Self-Assembly of two Sugar Based Surfactants. *J. Phys. Chem. B* **2009**, *113*, 7178−7187.
(20) Molina-Bolívar, J. A.; Hierrezuelo, J. M.; Ruiz, C. C. Self-Assembly, Hydration, and Structures in *N*-Decanoyl-*N*-Methylglucamide Aqueous Solutions: Effect of Salt Addition and Temperature. *J. Colloid Interface Sci.* **2007**, *313*, 656−664.
(21) Miyagishi, S.; Okada, T.; Asakawa, T. Salt Effect on Critical Micelle Concentrations of Nonionic Surfactants, *N*-Acyl-*N*-Methylglucamides (MEGA-*n*). *J. Colloid Interface Sci.* **2001**, *238*, 91−95.
(22) Okawauchi, M.; Hagio, M.; Ikawa, Y.; Sugihara, G.; Murata, Y.; Tanaka, M. Static Light Scattering Study of the Effect of Temperature on Micelle Formation of N-Alkanoyl-N-Methylglucamines in Aqueous Solutions. *Bull. Chem. Soc. Jpn.* **1987**, *60*, 2718−2725.
(23) Prasad, M.; Chakraborty, I.; Rakshit, A. K.; Moulik, S. P. Critical Evaluation of Micellization Behavior of Nonionic Surfactant MEGA-10 in Comparison with Ionic Surfactant Tetradecyltriphenylphosphonium Bromide Studied By Microcalorimetric Method in Aqueous Medium. *J. Phys. Chem. B* **2006**, *110*, 9815−9821.
(24) Basu Roy, G.; Chakraborty, I.; Ghosh, S.; Moulik, S. P. On Mixed Binary Surfactant Systems Comprising MEGA-10 and Alkyltrimethylammonium Bromides: A Detailed Physicochemical Study with a Critical Analysis. *J. Colloid Interface Sci.* **2007**, *307*, 543−553.
(25) Hierrezuelo, J. M.; Aguiar, J.; Ruiz, C. C. Stability, Interaction, Size and Microenvironmental Properties of Mixed Micelles of Decanoyl-N-Methylglucamide and Sodium Dodecyl Sulfate. *Langmuir* **2004**, *20*, 10419−10426.
(26) Sulthana, S.; Rao, P. V. C.; Bhat, S. G. T.; Nakano, T. Y.; Sugihara, G.; Rakshit, A. K. Solution Properties of Nonionic Surfactants and their Mixtures: Poly(Oxyethylene (10)) Alkyl Ether [C_nE_{10}] And MEGA-10. *Langmuir* **2000**, *16*, 980−987.
(27) Hierrezuelo, J. M.; Aguiar, J.; Ruiz, C. C. Role of the Head Group on the Mixed Micellization Process in Binary Systems Containing a Sugar-Based Surfactant: Decanoyl- N -Methylglucamide. *Mol. Phys.* **2005**, *103*, 3299−3308.
(28) Walter, A.; Suchy, S. E.; Vinson, P. K. Solubility Properties of the Alkylmethylglucamide Surfactants. *Biochim. Biophys. Acta* **1990**, *1029*, 67−74.
(29) Hildreth, J. E. K. N-D-Gluco-N-Methyalkanamide Compounds, a New Class of Nonionic Detergent for Membrane Biochemistry. *Biochem. J.* **1982**, *207*, 363−366.
(30) Hanatani, M.; Nishifuji, K.; Futai, M.; Tsuchiya, T. Solution and Reconstitution of E. Coli Membrane Proteins with Alkanoyl-N-Methylglucamides. *J. Biochem.* **1984**, *95*, 1349−1353.
(31) Lakowicz, J. R. *Principles of Fluorescence Spectroscopy*, 3rd ed.; Kluwer Academics/Plenum Publisher: New York, 2006.
(32) Aguiar, J.; Carpena, P.; Molina-Bolívar, J. A.; Ruiz, C. C. On the Determination of the Critical Micelle Concentration by the Pyrene 1:3 Ratio Method. *J. Colloid Interface Sci.* **2003**, *258*, 116−122.
(33) Turro, N. J.; Yekta, A. Luminescent Probes for Detergent Solution. A Simple Procedure for Determination of the Mean Aggregation Number of Micelles. *J. Am. Chem. Soc.* **1978**, *100*, 5951−5952 and references therein..
(34) Karukstis, K. K.; McDonough, J. R. Characterization of the Aggregates of N-Alkyl-N-Methylpyrrolidinium Bromide Surfactants in Aqueous Solution. *Langmuir* **2005**, *21*, 5716−5721 and references therein..
(35) Majhi, P. R.; Moulik, S. P. Energetics of Micellization: Reassessment by High-Sensitivity Titration Microcalorimeter. *Langmuir* **1998**, *14*, 3986−3990 and references therein..
(36) (a) Naskar, B.; Dan, A.; Ghosh, S.; Moulik, S. P. Viscosity and Solubility Behavior of Polysaccharide Inulin in Water, Water + Dimethly Sulfoxide, and Water + Isopropanol Media. *J. Chem. Eng. Data* **2010**, *55*, 2424−2427. (b) Dan, A.; Ghosh, S.; Moulik, S. P. The Solution Behavior of Poly(Vinylpyrrolidone): Its Clouding in Salt Solution, Solvation by Water and Isopropanol, and Interaction with

Sodium Dodecyl Sulfate. *J. Phys. Chem. B* **2008**, *112*, 3617−3624 and references herein..

(37) (a) Behera, K.; Pandey, S. Ionic Liquid Induced Changes in the Properties of Aqueous Zwitterionic Surfactant Solution. *Langmuir* **2008**, *24*, 6462−6469. (b) Behera, K.; Om, H.; Pandey, S. Modifying Properties of Aqueous Cetyltrimethylammonium Bromide with External Additives: Ionic Liquid 1-Hexyl-3-Methylimmidazolium Bromide Versus Cosurfactant N-Hexyltrimethylammonium Bromide. *J. Phys. Chem. B* **2009**, *113*, 786−793. (c) Behera, K.; Pandey, S. Concentration Dependent Dual Behavior of Hydrophilic Ionic Liquid in Changing Properties of Aqueous Sodium Dodecyl Sulfate. *J. Phys. Chem. B* **2007**, *111*, 13307−13315. (d) Rai, R.; Baker, G. A.; Behera, K.; Mohanty, P.; Kurur, N. D.; Pandey, S. Ionic Liquid-Induced Unprecedented Size Enhancement of Aggregates within Aqueous Sodium Dodecylbenzene Sulfonate. *Langmuir* **2010**, *26*, 17821−17826. (e) Behera, K.; Pandey, S. Interaction Between Ionic Liquid and Zwitterionic Surfactant: A Comparative Study of two Ionic Liquids with Different Anions. *J. Colloid Interface Sci.* **2009**, *331*, 196−205.

(38) (a) Rao, V. G.; Ghatak, C.; Ghosh, S.; Pramanik, R.; Sarkar, S.; Mandal, S.; Sarkar, N. Ionic Liquid-Induced Changes in the Properties of Aqueous Cetyltrimethylammonium Bromide: A Comparative Study of two Protic Ionic Liquids with Different Anions. *J. Phys. Chem. B* **2011**, *115*, 3828−3837. (b) Pramanik, R.; Sarkar, S.; Ghatak, C.; Rao, V. G.; Mandal, S.; Sarkar, N. Effect of 1-Butyl-3-Methylimidazolium Tetrafluoroborate Ionic Liquid on Triton X-100 Aqueous Micelles: Solvent and Rotational Relaxation Studies. *J. Phys. Chem. B* **2011**, *115*, 6957−6963.

(39) (a) Behera, K.; Pandey, M. D.; Porel, M.; Pandey, S. Unique Role of Hydrophilic Ionic Liquid in Modifying Properties of Aqueous Triton X-100. *J. Chem. Phys.* **2007**, *127*, 184501. (1−10). (b) Behera, K.; Dahiya, P.; Pandey, S. Effect of Added Ionic Liquid on Aqueous Triton X-100 Micelles. *J. Colloid Interface Sci.* **2007**, *307*, 235−245.

(40) (a) Corrin, M. L.; Harkins, W. D. The Effect of Salts on the Critical Concentration for the Formation of Micelles in the Colloidal Electrolytes. *J. Am. Chem. Soc.* **1947**, *19*, 683−688. (b) Maeda, H. Some Thoughts Regarding Theoretical Aspects of the Corrin−Harkins Relation and the Micellization Product of Ionic Micelles. *J. Colloid Interface Sci.* **2001**, *241*, 18−25.

(41) Ruiz, C. C.; Bolívar, J. A. M.; Aguiar, J.; Maclsaac, G.; Moroze, S.; Palepu, R. Thermodynamic and Structural Studies of Triton X-100 Micelles in Ethylene Glycol-Water Mixed Solvents. *Langmuir* **2001**, *17*, 6831−6840.

(42) Molina-Bolivar, J. A.; Hierrezuelo, J. M.; Ruiz, C. C. Effect of NaCl on the Self-Aggregation of N-Octyl-B-D-Thioglucopyranoside in Aqueous Medium. *J. Phys. Chem. B* **2006**, *110*, 12089−12095.

(43) Ruiz, C. C.; Bolívar, J. A. M.; Aguiar, J.; Maclsaac, G.; Moroze, S.; Palepu, R. Effect of Ethylene Glycol on the Thermodynamic and Micellar Properties of Tween 20. *Colloid Polym. Sci.* **2003**, *281*, 531−541.

(44) Oda, H.; Nagadome, S.; Lee, S.; Ohseto, F.; Sakai, Y.; Sugihara, S. Thermodynamic Study on Micelle Formation of N-Nonyl-B-D-Thiomaltoside in Water and Water/Alcohol Mixtures and on Adsorption at Air/Water Interface: A Study Performed By Comparing with MEGA-10 and Alkyl Glucosides. *J. Surf. Sci. Technol.* **1998**, *14*, 1−22.

(45) (a) Sulthana, S. B.; Bhat, S. G. T.; Rakshit, A. K. Studies of the Effect of Additives on the Surface and Thermodynamic Properties of Poly(Oxyethylene(10)) Lauryl Ether in Aqueous Solution. *Langmuir* **1997**, *13*, 4562−4568. (b) Rosen, M. J.; Mathias, J. H.; Davenport, L. Aberrant Aggregation Behavior of Cationic Gemini Surfactants Investigated by Surface Tension, Interfacial Tension, and Fluorescence Method. *Langmuir* **1999**, *15*, 7340−7346. (c) Rehfeld, S. J. Adsorption of Sodium Dodecyl Sulfate at Various Water-Hydrocarbon Interfaces. *J. Phys. Chem.* **1967**, *71*, 738−745.

(46) (a) Burczyk, B.; Wilk, K. A.; Sokolowski, A.; Syper, L. Synthesis And Surface Properties of *N*-Alkyl-*N*-Methylgluconamides and *N*-Alkyl-*N*-Methyllactobionamides. *J. Colloid Interface Sci.* **2001**, *240*, 552−558. (b) Eastoe, J.; Nave, S.; Downer, A.; Paul, A.; Rankin, A.; Tribe, K.; Penfold, J. Adsorption of Ionic Surfactants at the Air-Solution Interface. *Langmuir* **2000**, *16*, 4511−4518.

(47) Chatterjee, A.; Sanyal, S. K.; Mishra, B. K.; Puri, P. M.; Moulik, S. P. Thermodynamics of Micelle Formation of Ionic Surfactants: A Critical Assessment for Sodium Dodecyl Sulfate, Cetyl Pyridinium Chloride and Dioctyl Sulfosuccinate (Na Salt) by Microcalorimetric, Conductometric, and Tensiometric Measurements. *J. Phys. Chem. B* **2001**, *105*, 12823−12831 and references therein..

(48) (a) Moulik, S. P.; Mitra, D. Amphiphile Self-Aggregation: An Attempt to Reconcile the Agreement-Disagreement Between the Enthalpies of Micellization Determined by the van't Hoff and Calorimetry Methods. *J. Colloid Interface Sci.* **2009**, *337*, 569−578. and references therein. (b) Horn, J. R.; Brandts, J. F.; Murphy, K. P. van't Hoff and Calorimetric Enthalpies II: Effect of Linked Equilibria. *Biochemistry* **2002**, *41*, 7501−7507. (c) Chaires, J. B. Calorimetry and Thermodynamics in Drug Design. *Annu. Rev. Biophys.* **2008**, *37*, 135−151. (d) Fisicaro, E.; Compari, C.; Duce, E.; Biemmi, M.; Peroni, M.; Braibanti, A. Thermodynamics of Micelle Formation in Water, Hydrophobic Process and Surfactant Self-Assemblies. *Phys. Chem. Chem. Phys.* **2008**, *10*, 3903−3914.

(49) Corkill, J. M.; Goodman, J. F.; Harrold, S. P. Thermodynamics of Micellization of Non-Ionic Detergents. *Trans. Faraday Soc.* **1964**, *60*, 202−207.

(50) Moroi, Y. *Micelles: Theoretical and Applied Aspects*; Plenum Press: New York, 1992.

(51) (a) Kresheck, S. C. The Temperature dependence of the Heat Capacity Change for Micellization of Nonionic Surfactants. *J. Colloid Interface Sci.* **2006**, *298*, 432−440. (b) Kresheck, S. C. Isothermal Titration Calorimetry Studies of Neutral Salt Effects on the Thermodynamics of Micelle Formation. *J. Phys. Chem. B* **2009**, *113*, 6732−6735. (c) Menger, F. M. The Structure of Micelles. *Acc. Chem. Res.* **1979**, *12*, 111−117. (d) Menger, F. M.; Jerkuncia, J. M.; Johnston, J. C. The Water Content of Micelle Interior. The Fjord Vs. Reef Models. *J. Am. Chem. Soc.* **1978**, *100*, 4676−4678. (e) Clifford, J. Properties of Micellar Solutions. Part 4-Spin Lattice Relaxation Times of Hydrocarbon Chain Protons in Solutions of Sodium Alkyl Sulfates. *Trans. Faraday Soc.* **1965**, *61*, 1276−1282.

(52) (a) Thomas, J. K. Radiation-Induced Reactions in Organized Assemblies. *Chem. Rev.* **1980**, *80*, 283−299. (b) Slavik, J. Anilinonaphthalene Sulfonate as a Probe of Membrane Composition and Function. *Biochim. Biophys. Acta* **1982**, *694*, 1−25. (c) Nanjo, D.; Hosoi, H.; Fujino, T.; Tahara, T.; Korenaga, T. Femtoseceond/Picoseconds Time-Resolved Fluorescence Study of the Hydrophilic Polymer Fine Particles. *J. Phys. Chem. B* **2007**, *111*, 2759−2764.

(53) (a) Kalyanasundaram, K. *Photophysical Chemistry in Micro-heterogeneous Systems*; Acedemic Press: New York, 1987. (b) Kalyana-sundaram, K.; Thomas, J. K. Environmental Effects on the Vibronic Band Intensities in Pyrene Monomer Fluorescence and Their Application in Studies of Micellar Systems. *J. Am. Chem. Soc.* **1977**, *99*, 2039−2044.

(54) Hazra, P.; Chakrabarty, D.; Sarkar, N. Solvation Dynamics of Coumarin 153 in Aqueous and Non-Aqueous Reverse Micelles. *Chem. Phys. Lett.* **2003**, *371*, 553−562.

(55) (a) Dutt, G. B. Are the Experimentally Determined Micro-viscosities of Micelles Probe Dependent? *J. Phys. Chem. B* **2004**, *108*, 3651−3657. (b) Dutt, G. B. Rotational Relaxation of Nondipolar Probes in Triton X-100 Micelle in the Presence of Added Salt: Correlation of Lateral Diffusion Coefficient with "Dry" Micelle Radius. *J. Phys. Chem. B* **2003**, *107*, 3131−3136. (c) Dutt, G. B. Rotational Diffusion of Nondipolar Probes in Triton X-100 Micelles: Role of Specific Interactions and Micelle Size on Probe Dynamics. *J. Phys. Chem. B* **2002**, *106*, 7398−7404. (d) Dutt, G. B. Rotational Diffusion of Hydrophobic Probes in Brij-35 Micelles: Effect of Temperature on Micellar Internal Environment. *J. Phys. Chem. B* **2003**, *107*, 10546−10551.

(56) (a) Kumbhakar, M.; Goel, T.; Mukerjee, T.; Pal, H. Role of Micellar Size and Hydration on Solvation Dynamics: A Temperature Dependent Study in Triton X-100 and Brij-35 Micelles. *J. Phys. Chem. B* **2004**, *108*, 19246−19254. (b) Kumbhakar, M.; Nath, S.; Mukherjee,

T.; Pal, H. Solvation Dynamics in Triton X-100 and Triton X-165 Micelles: Effect of Micellar Size and Hydration. *J. Chem. Phys.* **2004**, *121*, 6026−6033. (c) Kumbhakar, M.; Mukherjee, T.; Pal, H. Temperature Effect on the Fluroescence Anisotropy Decay Dynamics of Coumarin-153 Dye in Triton X-100 and Brij-35 Micellar Solutions. *Photochem. Photobiol.* **2005**, *81*, 588−594. (d) Kumbhakar, M.; Goel, T.; Mukherjee, T.; Pal, H. Effect of Lithium Chloride on the Palisade Layer of the Triton X-100 Micelle: Two Sites for Lithium Ions as Revealed by Solvation and Rotational Dynamics Studies. *J. Phys. Chem. B* **2005**, *109*, 18528−18534. (e) Kumbhakar, M. Effect of Ionic Surfactants on the Hydration Behavior of Triblock Copolymer Micelles: A Solvation Dynamics Study of Coumarin 153. *J. Phys. Chem. B* **2007**, *111*, 12154−12161. (f) Goel, T.; Kumbhakar, M.; Mukherjee, T.; Pal, H. Effect of Sphere to Rod Transition on the Probe Microenvironment in Sodium Dodecyl Sulphate Micelles: A Time Resolved Fluorescence Anisotropy Study. *J. Photochem. Photobiol. A* **2010**, *209*, 41−48.

(57) Horng, M. L.; Gardecki, J. A.; Papazyan, A.; Maroncelli, M. Subpicosecond Measurements of Polar Solvation Dynamics: Coumarin 153 Revisited. *J. Phys. Chem.* **1995**, *99*, 17311−17337.

(58) (a) Reynolds, L.; Gardecki, J. A.; Frankland, S. J. V.; Horng, M. L.; Maroncelli, M. Dipole Solvation in Nondipolar Solvents: Experimental Studies of Reorganization Energies And Solvation Dynamics. *J. Phys. Chem.* **1996**, *100*, 10337−10354. (b) Jones, G. G., II; Jackson, W. R.; Choi, C. Y.; Bergmark, W. R. Solvent Effects on Emission Yield and Lifetime for Coumarin Laser Dyes. Requirements for a Rotatory Decay Mechanism. *J. Phys. Chem.* **1985**, *89*, 294−300. (c) Bhattacharyya, K.; Bagchi, B. Slow Dynamics of Constrained Water in Complex Geometries. *J. Phys. Chem. A* **2000**, *104*, 10603−10613.

(59) (a) Lianos, P.; Viriot, M. L.; Zana, R. Study of the solubilization of Aromatic Hydrocarbons by Aqueous Micellar Solutions. *J. Phys. Chem.* **1984**, *88*, 1098−1101. (b) Zana, R. In *Surfactant Solutions: New Method of Investigation*; Zana, R., Ed.; Dekker: New York, 1980; p 241.

(60) Ghatak, C.; Rao, V. G.; Pramanik, R.; Sarkar, S.; Sarkar, N. The Effect of Membrane Fluidity on FRET Parameters: An Energy Transfer Study Inside Small Unilamellar Vesicle. *Phys. Chem. Chem. Phys.* **2011**, *13*, 3711−3720.

(61) (a) Paul, B. K.; Guchhait, N. Exploring the Strength, Mode, Dynamics, and Kinetics of Binding Interaction of a Cationic Biological Photosensitizer with DNA: Implication on Dissociation of the Drug−DNA Complex Via Detergent Sequestration. *J. Phys. Chem. B* **2011**, *115*, 11938−11949. (b) Paul, B. K.; Samanta, A.; Guchhait, N. Modulated Photophysics of an ESIPT Probe 1-Hydroxy-2-Naphthaldehyde Within Motionally Restricted Environments of Liposome Membranes Having Varying Surface Charges. *J. Phys. Chem. B* **2010**, *114*, 12528−12540. (c) Paul, B. K.; Guchhait, N. Constrained Photophysics of an ESIPT Probe Within β-Cyclodextrin Nanocavity and Chaotrope-Induced Perturbation of the Binding Phenomenon: Implication Towards Hydrophobic Interaction Mechanism Between Urea and the Molecular Probe. *J. Colloid Interface Sci.* **2011**, *353*, 237−247. (d) Paul, B. K.; Guchhait, N. Spectral Deciphering of the Interaction Between an Intramolecular Hydrogen Bonded ESIPT Drug, 3,5-Dichlorosalicylic acid, and a Model Transport Protein. *Phys. Chem. Chem. Phys.* **2012**, *14*, 8892−8902. (e) Paul, B. K.; Guchhait, N. Modulation of Prototropic Activity and Rotational Relaxation Dynamics of a Cationic Biological Photosensitizer Within the Motionally Constrained Bio-Environment of a Protein. *J. Phys. Chem. B* **2011**, *115*, 10322−10334.

(62) Ruiz, C. C. Rotational Dynamics of Coumarin 153 in Non-ionic Mixed Micelles of *N*-Octyl-β-D-Thioglucoside and Triton X-100. *Photochem. Photobiol. Sci.* **2012**, *11*, 1331−1338.

(63) Valeur, B. *Molecular Fluorescence: Principles and Applications*; Wiley-VCH: New York, 2002.

(64) Cross, J. A.; Fleming, G. Analysis of Time-Resolved Fluorescence Anisotropy Decays. *Biophys. J.* **1984**, *46*, 45−56.

(65) (a) Sahu, K.; Mondal, S. K.; Ghosh, S.; Roy, D.; Bhattacharyya, K. Temperature Dependence of Solvation Dynamics and Anisotropy Decay in a Protein: ANS in Bovine Serum Albumin. *J. Chem. Phys.* **2006**, *124*, 124909. (b) Mitra, R. K.; Sinha, S. S.; Pal, S. K. Temperature-Dependent Hydration at Micellar Surface: Activation Energy Barrier Crossing Model Revisited. *J. Phys. Chem. B* **2007**, *111*, 7577−7583 and references therein.

(66) (a) Becke, A. D. Density-Functional Thermochemistry. III. The Role of Exact Exchange. *J. Chem. Phys.* **1993**, *98*, 5648−5652. (b) Frisch, M. J.; Trucks, G. W.; Schlegel, H. B.; Scuseria, G. E.; Robb, M. A.; Cheeseman, R. J., Jr. Montgomery, J. A.; Vreven, T.; Kudin, K. N.; Burant, J. C. et al. *Gaussian 03, Revision E.01*; Gaussian, Inc.: Wallingford, CT, 2004.

(67) Sheng, X. W.; Mentel, L.; Gritsenko, O. V.; Baerends, E. J. Counterpoise Correction is not Useful for Short and Van der Waals Distances but may be Useful at Long Range. *J. Comput. Chem.* **2011**, *32*, 2896−2901.

(68) (a) Weimann, M.; Fárník, M.; Suhm, M.; E Alikhani, M.; Sadlej, J. Cooperative and Anticooperative Mixed Trimers of HCl and Methanol. *J. Mol. Struct.* **2006**, *790*, 18−26. (b) Masella, M.; Flament, J. P. A Theoretical Study of Five Water/Ammonia/Formaldehyde Cyclic Trimers: Influence of Cooperative Effects. *J. Chem. Phys.* **1999**, *110*, 7245−7255. (c) Das, D.; Dey, J.; Chandra, A. K.; Thapa, U.; Ismail, K. Aggregation Behavior of Sodium dioctylsulfosuccinate in Aqueous Ethylene Glycol Medium. A Case of Hydrogen Bonding Between Surfactant and Solvent and its Manifestation in the Surface Tension Isotherm. *Langmuir* **2012**, *28*, 15762−15769.

(69) Hobza, P.; Bludsky, O.; Suhai, S. Reliable Theoretical Treatment of Molecular Clusters: Counterpoise-Corrected Potential Energy Surface and Anharmonic Vibrational Frequencies of the Water Dimer. *Phys. Chem. Chem. Phys.* **1999**, *1*, 3073−3078.